

# Flood-risk assessment in urban environment by geospatial approach: a case study of Ambala City, India

Surjit Singh Saini<sup>1</sup> · S. P. Kaushik<sup>1</sup> · Ravinder Jangra<sup>1</sup>

Received: 5 December 2015 / Accepted: 26 July 2016 / Published online: 16 August 2016  
© Società Italiana di Fotogrammetria e Topografia (SIFET) 2016

**Abstract** Looking at land use and functional structure characteristics, floods in urban environment are costlier and difficult to manage than in rural environment. In India, flooding is an inevitable problem for several cities. In the state of Haryana, Ambala City has a long history of serious flooding problem. Based on primary as well as secondary data, the present study attempts to examine the natural and anthropogenic causes of flooding on catchment and city scale. Geographic Information System (GIS)-based flood-risk modeling and consequences of flooding are presented for the selected most critical zone. Based on the past 21-year maximum discharge data of the Tangri River, flood probability is calculated for a 2-, 5-, 10-, and 20-year return period using *Weibull's plotting position* formula, and the likely maximum discharge of 500, 1000, 1200, and 1500 m<sup>3</sup>, respectively, is used for the prediction of flood extent using Hydraulic Engineering Center-River Analysis System (HEC-RAS) software. Flood depth is calculated by employing spatial interpolation method using observed flood depth samples. Model result revealed that the flood inundation areas are 690, 1135, 1530, and 2300 ha, respectively, and accordingly likely impact on land use and population are assessed. The modeled 5-year return flood extents were validated using the observed data of the latest flood event in July 2010, including remote

sensing imagery and field survey. Hence, in order to mitigate adverse impact of flooding in urban environment, such output can be used by urban local bodies, town planners, and policy makers to support decision-making in risk-sensitive land use planning by integrating climate change scenarios.

**Keywords** GIS · Risk · Return period · Peak flow

## Introduction

Flooding is part of the earth's natural hydrologic cycle and has been occurring since ages. Among all the natural disasters, floods are most repeated natural catastrophe occurring in one or other parts of the world every year. Over time, floods are slowly converted into flood hazard, primarily due to occupancy of incompatible anthropogenic activities in flood plains. Otherwise, floods rejuvenate groundwater aquifers and help to keep the floodplains fertile by depositing rich silt on land adjoining rivers/streams (United Nations International Strategy for Disaster Reduction 2009).

It is broadly agreed that flood risk is a function of hazard, exposure, vulnerability, adaptive, and resilience capacity. With this theoretical base, flood threat is defined as the incidence of a hydrologic flood occasion with a given probability, whereas, exposure to combination of anthropogenic factors make it a flood hazard affecting local communities and its belongings (Alexander 1991; UN DHA 1992; Helm 1996; Smith 1996; Stenchion 1997; Crichton 1999; Kron 2005; Buchele et al. 2006).

Asian countries are most frequently affected with high intensity of floods particularly by riverine floods; although the number of human lives lost has decreased, in terms of economic losses, its impact on population, agriculture, and infrastructure has increased significantly. However, despite

✉ Surjit Singh Saini  
saini.surjit@gmail.com

S. P. Kaushik  
spk34@rediffmail.com

Ravinder Jangra  
ravinderjangra13@gmail.com

<sup>1</sup> Department of Geography, Kurukshetra University,  
Kurukshetra, Haryana 136119, India

inevitable natural and hydro-meteorological factors, anthropogenic interventions through incompatible developments in floodplains are increasing flood risk and damage. Moreover, in recent years, several authors mentioned that floods are predicted to carry vast degrees of distress in the future, as a result of worldwide climatic change (Mirza 2002; Van Aalast 2006; IPCC 2007; Hirabayashi et al. 2008; Whitfield 2012).

With this view, considering land use and functional characteristics, in rural part, flooding can have larger social impact; whereas, floods are more expensive and unmanageable in urban environment due to complex concentration of population, socioeconomic activities, infrastructure, and assets (Jah et al. 2011). Generally, a large part of rainfall runoff is controlled by permeability characteristics of the soil, surface slope, and vegetal cover. Therefore, runoff directly relates to the proportion of the area covered by impervious surfaces. Johnson and Sayre (1973), Dempster (1974), and National Disaster Management (2010) recognized that flood peaks rise about 1.8 to 9 times and flood volume up to 6 times in urban areas against rural ones.

India has been experiencing floods of varying intensity every year occurring in one or other parts of the country at a time. It is estimated that around 40 million hectares (12 %) of the country's land area is prone to floods, and on an average, eight million people are affected by floods every year (Purba et al. 2006). Since 2000, increasing trend of urban flooding has been reported in India and several main cities have been badly affected. These cities include Hyderabad in 2000, Ahmedabad in 2001, Delhi in 2002 and 2003, Chennai in 2004, Mumbai in 2005, Surat in 2006, Kolkata in 2007, Jamshedpur in 2008, Delhi in 2009, and Guwahati and Delhi in 2010 (Patil 2015). Recent flooding in urban environment has been reported from Jaipur in 2012, Srinagar in 2014, Kolkata in 2015, and the most recent (on November 2015) widespread flooding in Tamil Nadu had devastating effects on several towns including Chennai, Puducherry, Kancheepuram, and Cuddalore (Skymet Weather Report 2015).

In India, with special reference to urban flooding, adequate attention was given after the Mumbai floods of July 2005. Hence, there is an increasing interest in modeling flood risk to adopt suitable strategies to minimize the damage and manage the surplus flood water as a resource. National Disaster Management Authority (NDMA) has taken initiative to address urban flooding as a separate type of disaster and formulated the Flood Guidelines in 2006, released in 2008 (National Disaster Management 2010). Looking at increasing urbanization trends and uncertainties of climatic events, it is perceived that over time flood damage in urban environment is likely to increase many fold (Kates and Wilbanks 2003). Describing the unprecedented heavy rainfall in Tamil Nadu and Jammu and Kashmir in 2014 as instances of climate change episodes,

environmentalists warned the urban planners towards immediate enactment of flood plain zoning and building by-laws in order to stop unplanned development and to minimize losses to life and infrastructure due to natural hazards (The Tribune 2015). A flood plain zoning bill was prepared by the Government of India in 1975, aimed at minimizing losses resulting from occurrence of natural hazards. However, to some extent, Manipur and Rajasthan states have enacted this bill, but no other state government has done this so far (Kumar et al. 2005). In order to implement flood plain zoning measure, one of the major requirements is availability of large-scale maps to demarcate flood-prone areas. Therefore, using remote sensing, hydro-meteorological, topographical, and land use data, geospatial approach can be effectively used to assess flood risk of different magnitudes, and accordingly mapping of hazard zones (low, medium, high). The output of this approach can be used to regulate risk-sensitive land use and to avoid incompatible development in floodplain while preparing for a perspective development plan for the city.

Several mathematical models integrated with Geographic Information System (GIS) perform well in flood-risk modeling and hazard-zone mapping. These studies have been carried out in GIS environment, integrated with specific hydrologic modeling software/tools such as HEC-HMS, Hydraulic Engineering Center-River Analysis System (HEC-RAS), HEC-Geo RAS (USACE 2002), Arc Hydro (ESRI 2005), and MIKE (DHI 2009). These flood-risk models required specific input data, in a spatial context which mainly includes digital elevation model (DEM), watershed boundary, main channel's maximum length, channel/floodplain roughness coefficients, cross-sections, river channel left/right boundary, soils, land use, and rainfall/discharge data. These models have two main components namely, a hydrologic modeling which estimates the runoff from the rainfall/discharge, and, a hydraulic model which assesses the flood inundation profiles at locations of interest along the stream (Arora et al. 2001). The modeling output includes the flood hazard/risk map against different probability/return period that presents three aspect of flooding such as *water depth, duration, and spatial extent*. Based on these aspects, flood zone maps of varying intensities (high, medium, low) are prepared in 2D/3D visual representation. Finally, flood-risk modeling results are generally overlaid/combined with different themes such as existing or proposed land uses, population, public/private infrastructure, etc. in order to assess the likely damage and vulnerability and accordingly recommend mitigating measures (Islam and Sado 2000; Tralli et al. 2005; Pappenberger et al. 2005; Casas et al. 2006; Wright et al. 2008; Salimi et al. 2008; Patro et al. 2009; Aphrodite 2010; Kute et al. 2014). In the state of Haryana, Ambala City is highly vulnerable to floods on account of its topography, climatic conditions, site and situation, and various other important man-made causes. Due to its proximity to Shiwalik hills (high slope), this city has invariably

experienced flash floods whenever there is heavy downpour at the upper stream area (Ambala District Disaster Management Plan (DDMP) 2015). This city has experienced major floods on an average of 4- to 5-year return period with variation in magnitudes and extents. The floods which occurred in September 1993, August 1995, July 2001, August 2002, August 2004, and July 2010 were the prominent ones experienced by the city (Ambala District Disaster Management Plan 2015). Although the city has experienced high-magnitude floods during 1995 and 2001, economic losses were severe during the flood that occurred in July 2010 (Department of Revenue and Disaster Management, Government of Haryana, Ambala District Disaster Management Plan 2015). Due to recent flooding, huge economic losses have been reported covering direct and indirect damage to public and private infrastructure, transport and communication interruption, post-flood disease, and the like. Recently, some protective and preventive measures have been taken up by the city administration towards the city side to combat the floods (Ambala District Disaster Management Plan 2012). Despite these measures, flooding situation remains the same largely due to anthropogenic factors, besides the inevitable natural factors. Thus, due to uncertainty of changing climate, flood-prone areas need to be examined in light of the existing as well as

future expansion of urban settlements. Hence, the present study has put efforts to systematically examine the issues and causes of flooding in urban environment by integrating hydro-meteorological, physiographic, and land use to analyze the potential flood risk and its impact on land use and local communities in the selected most critical areas of Ambala City.

## Study area description

### Regional setting

Ambala is located at  $30^{\circ} 20' 12.56''$  latitude and  $76^{\circ} 51' 46.94''$  longitude (Fig. 1), about 205 km from New Delhi (National Capital) and 45 km from the State Capital (Chandigarh). The average height of the study area is 277 m above sea level (asl). Ambala area experiences an annual average rainfall of 1197.86 mm, out of which about 70 % is received during the south-west monsoon period, July to September (Khan 2007). It is well connected by highways and railways and gateway to the neighboring states of Punjab, Himachal Pradesh, and Jammu and Kashmir. Hence, these characteristics make this study more important in order

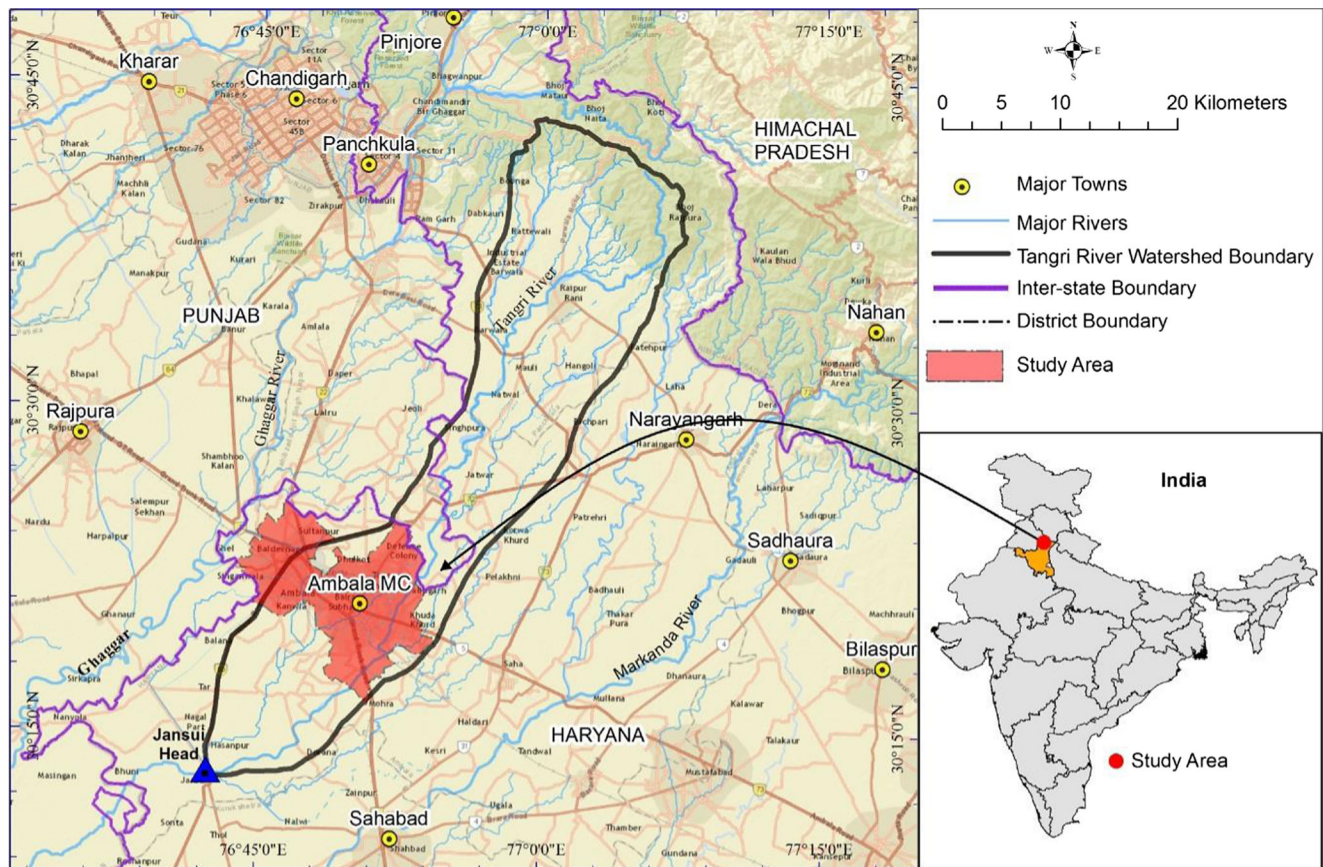


**Fig. 1** Study area (Ambala Municipal Corporation) location and its regional setting (ESRI Online Base Map 2014)

for transport of people, goods, and services across the state border to not be interrupted by flooding. The Tangri River is one significant tributary of the main Ghaggar River and surges through the study area. It originates from the Morni Hills of Shivalik Ranges of Lower Himalaya. This seasonal stream has abundant water during monsoon period and swells many times to cause floods and create havoc. The Catchment of the Tangri River is located between River Markanda (east) and River Ghaggar (west), as shown in Fig. 1. The Tangri River is relatively straight and initially steep. Its headwater starts at an elevation of 1200 m asl up to 8 km, traversing through Shivalik hills, and thereafter levels abruptly down to 400 m asl at foot hills of Shivalik, and then traverses a distance of 40 km with gently undulating slope up to the Ambala City settlement area.

### Ambala City profile

Each town has its own constraint or potential that is responsible for present and the future growth, which is mainly determined by the geography, history, and economy of the town (Toutain and Gopiprasad 2006). In case of Ambala City, there are many natural and man-made

physical barriers affecting its expansion on all sides. There are three railway tracks that pass through town; while on one hand the excellent rail linkages of the towns have promoted the economic growth, on the other hand, these have become major barrier in physical integration of all sub-areas. Similarly, in case of natural barriers, the Tangri River passes on the eastern side of Ambala Cantonment while the Ghaggar River flows on the western side (Ambala Draft Development Plan (DDP) 2025 2012). Presently, Ambala City is governed by Municipal Corporation. It has spread over an area of 133.96 km<sup>2</sup> and comprised three statutory towns, namely Ambala City, Ambala Cantonment, and Ambala Sadar, as shown in Fig. 2. Although Ambala cantonment is a separate statutory body and natural runoff does not follow man-made boundary, this area also has been included in the study. In addition, Ambala Municipal Corporation includes seven census towns located on the outskirts of all the sub-areas (Census of India 2011). Due to outgrowth, these sub-areas have merged to form one contiguous urban agglomeration (Ambala Draft Development Plan (DDP) 2025 2012). Population and area breakup of the settlements under the jurisdiction of Ambala

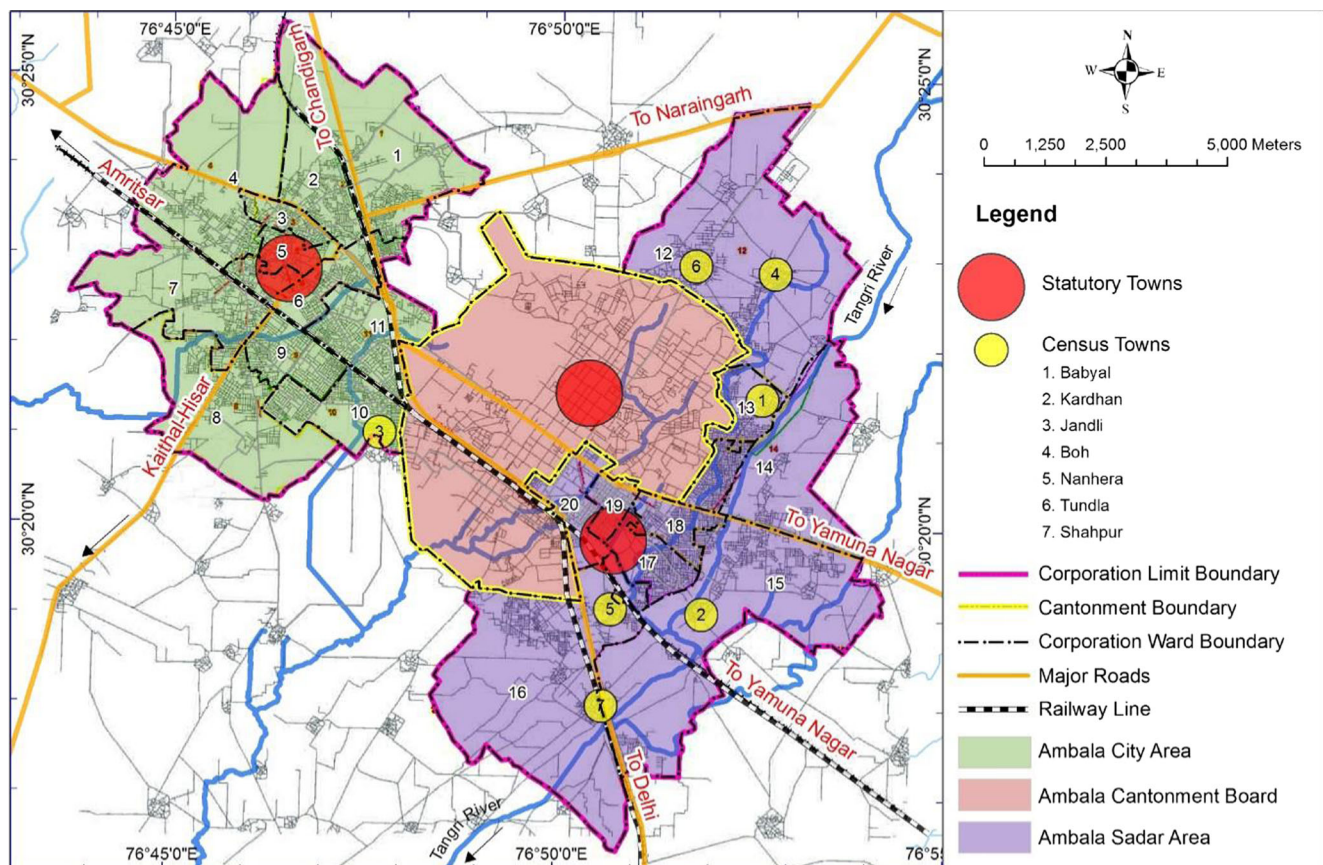


**Fig. 2** Administrative sub-areas in Ambala City (Ambala Municipal Corporation 2012; Census of India 2011)

**Table 1** Ambala Municipal Corporation: areas and population (Census of India 2011)

Sub-area	Sub-area description	Population	Area (ha)
Ambala City (Municipal Corporation)	Ambala City (statutory town)	195,153	4492.287 (33.53 %)
	Jandli Census Town	14,397	
	Sub-total	212,953 (47.61 %)	
Ambala Cantonment	Ambala Cantonment Board (statutory town)	55,370 (12.58 %)	3278.165 (24.47 %)
	Sub-total	55,370 (12.58 %)	
Ambala Sadar <sup>a</sup> (Municipal Corporation)	Ambala Sadar (statutory town)	103,093	5625.669 (41.99 %)
	Babiyal Census Town	26,412	
	Kardhan Census Town	18,662	
	Boh Census Town	8,482	
	Nanhera Census Town	6,035	
	Tundla Census Town	5,658	
	Kanwla Census Town	5,024	
	Sarasherri Village (outgrowth)	1,881	
	Sub-total	182,577 (39.81 %)	
Grand total		440,167 (100 %)	13,396.121 (100 %)

<sup>a</sup> Ambala Sadar area has been taken as case area for flood-risk modeling and impact assessment

Municipal Corporation is summarized in Table 1 (Census of India 2011).

The research team has digitized and analyzed a detailed existing land use map using high-resolution satellite images of base year 2010, available on Google Earth. The land use was examined, and it was found that the largest proportion of

total (10,117.96 ha) land excluding the Cantonment area (3278.165 ha) is covered by residential use (39 %) followed by agriculture/open (38 %), transportation (4.8 %), commercial (4.7 %), open space (4 %), public and semipublic (4 %), water bodies (3.7 %), and industrial use (1.6 %), as presented in Fig. 3

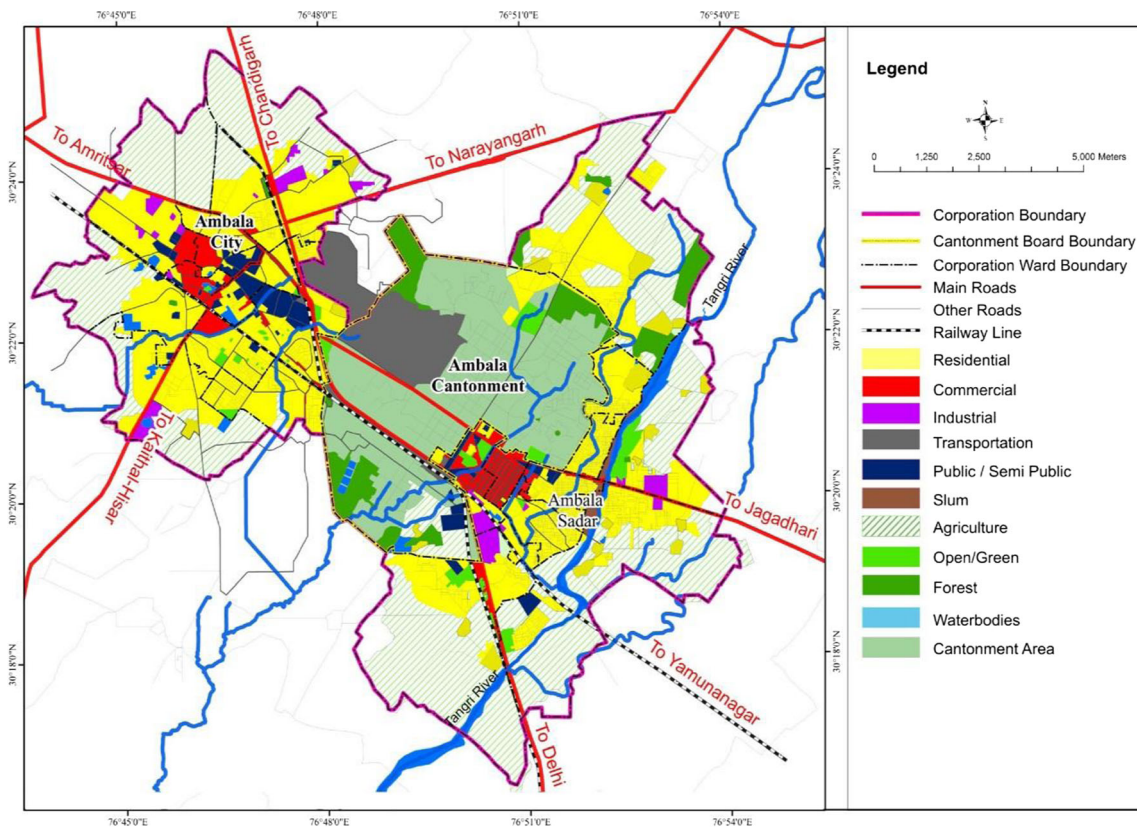
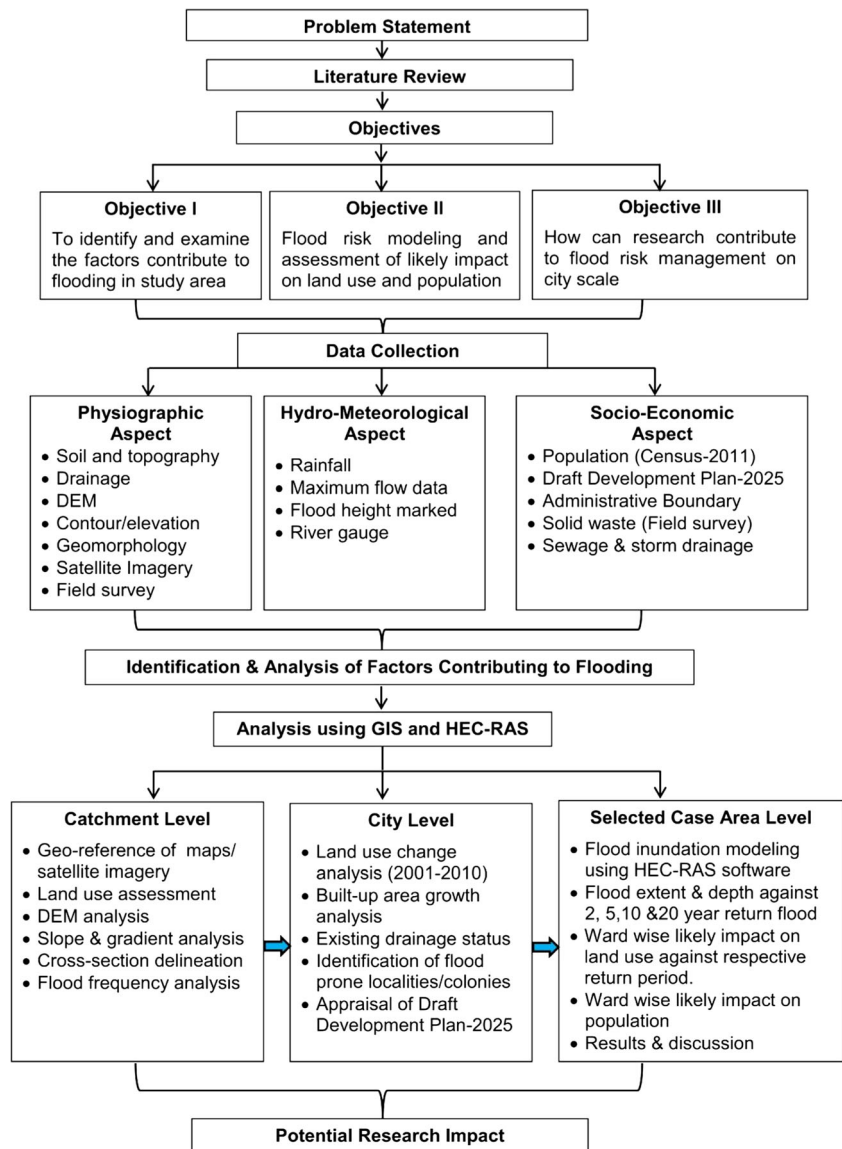


**Fig. 3** Land use map (2010) of Ambala City Municipal Corporation (Google Earth 2010)

**Fig. 4** Data base and methodology



## Data and approach

The present study is based on the data base and methodology for flood-risk assessment, as presented in Fig. 4

### Natural causes of flooding

Based on field investigation and secondary data, the following natural and anthropogenic factors at catchment and city level are examined to determine flood risk.

#### *Topography and proximity to high slope*

Most of the catchment area is flat, excluding the small hilly part falling in Siwalik Hills in the extreme north-

east. This hilly area is characterized by very undulating and steep slope with dissected rolling plain (HARSAC 1997). The research team examined the Cartosat-1 (30 m) DEM (National Remote Sensing Centre Hyderabad 2013) in GIS environment and found that ground elevation in the study area varies between 260 and 1120 m asl. The general slope is declining towards south-west with an average gradient of 1.5 m/km, but due to the high slope in the upper stream area, the rainfall water generally is not retained, and so it passes downstream and accumulates in the studied area. Hence, the city's proximity to high slope (Fig. 5) plays a very important role in creating surge and flash flooding (Ahlawat and Bansal 2010). Based on slope classification adopted from FAO (1990), we examined that the

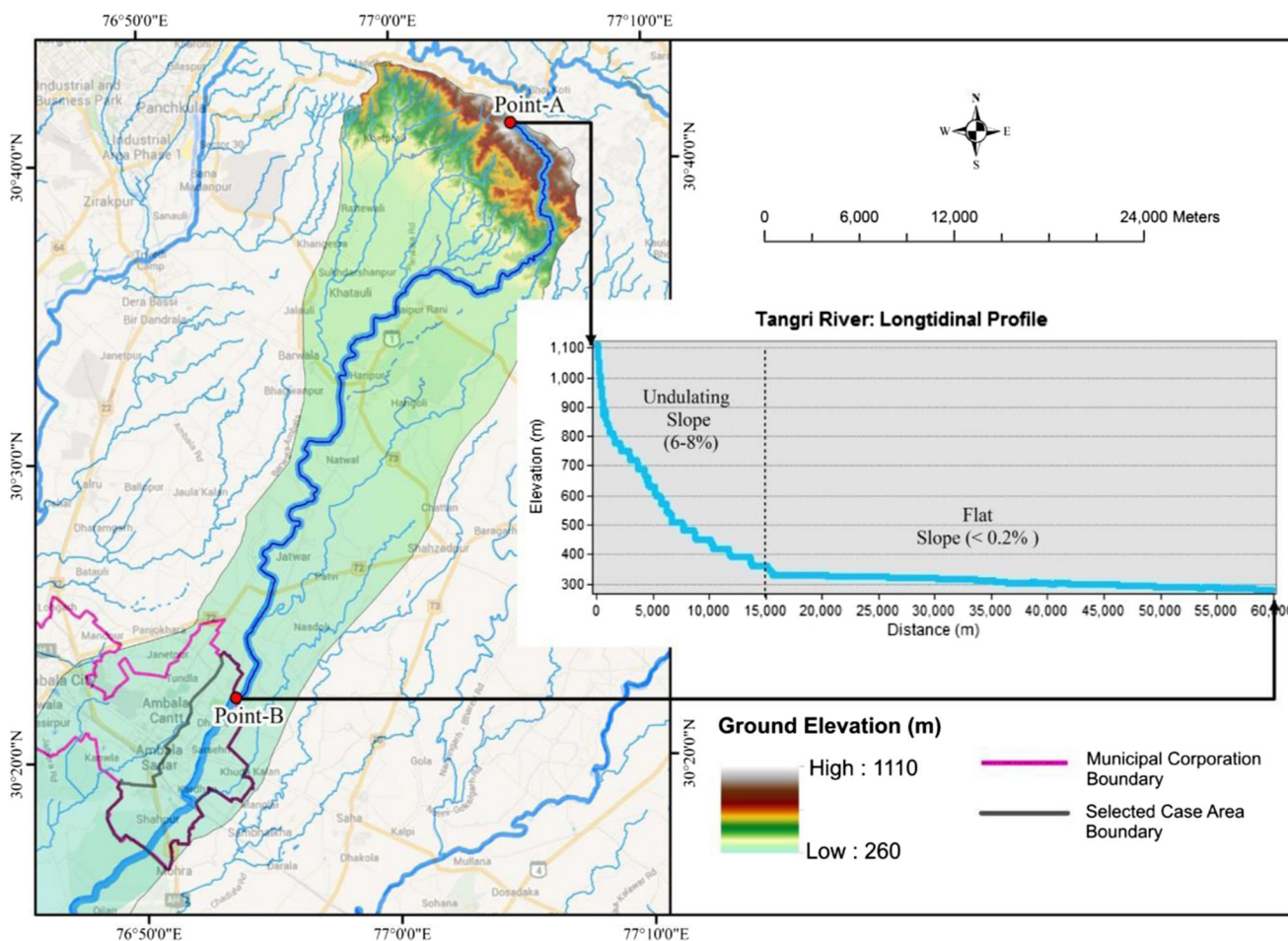


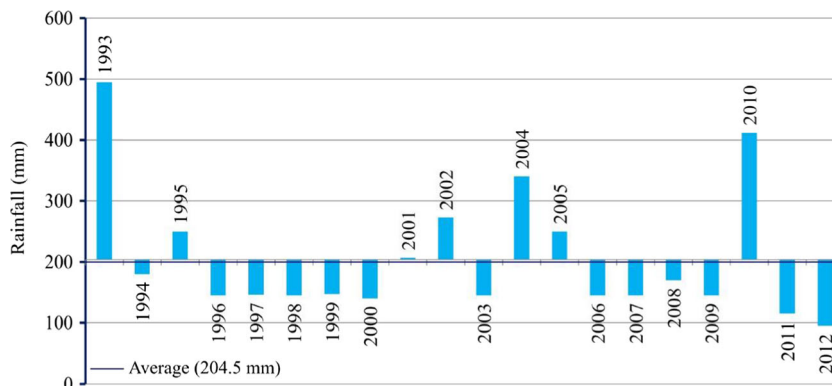
**Fig. 5** Tangri River: topography and longitudinal profile up to study area (Cartosat-1 DEM, National Remote Sensing Centre Hyderabad 2013)

main stream is flowing through an undulating slope (6–8 %) up to a distance of 15 km, and thereafter, abruptly comes down to a flat terrain (0.2 % slope). Consequently, the study area invariably experiences flash floods whenever there is high rainfall in the Shiwalik Hills.

*Prolonged high rainfall*

Although the average annual rainfall of the study area is 1105 mm, heavy rainfall for long period is the main cause of flooding (Irrigation Department Ambala 2012). Figure 6 displays maximum point rainfall

**Fig. 6** Maximum daily rainfall deviation from 20-year average (Irrigation Department Ambala 2012)



exceedances of the 20-year (1993–2012) average rainfall (204.5 mm). It is well evident that whenever daily rainfall was recorded at more than the 204.5 mm, the city will face a flooding problem. This generally occurred during south-west monsoon period (June–September).

#### *Soil erosion and silting of water channels*

Singh et al. (1992) clearly indicated that “Shiwalik region is composed of sandstone, grit, and conglomerates, with characters of fluvial deposits with deep soils, but slopes near the foothills contain pebbles and boulders, and these formations are geologically weak and unstable, resulting to these areas being highly vulnerable to soil erosion.” Hence, whenever high rainfall occurs in the upper stream area, flood water carries heavy silt which is deposited in the water channels. Consequentially, the channel’s bed level is rising, reducing flow carrying capacity, and making the channel vulnerable to overtopping during peak flow.

#### **Anthropogenic causes of flooding in urban areas**

There are many unsupportive land use activities developed in the catchment area, and how these activities play their role in urban flooding, is described hereafter;

#### *Influence of brick kiln industry*

Investment Climate (2010) reported that the construction sector found the fastest growing sector in the Chandigarh region. Consequently, in order to fulfill the structural and construction requirement for the industrial and housing projects in the fringe of Chandigarh, the upper catchment area of the River Tangri has experienced unconsolidated land fractures due to large number of brick kiln activities (Weber 2014). Based on field observation, the research team found that there are more than 60 brick kiln (Fig. 7) industrial units in operation, and area under fracture land was digitized and calculated in GIS environment which covers about 605 ha. These activities are causing loss of the natural small

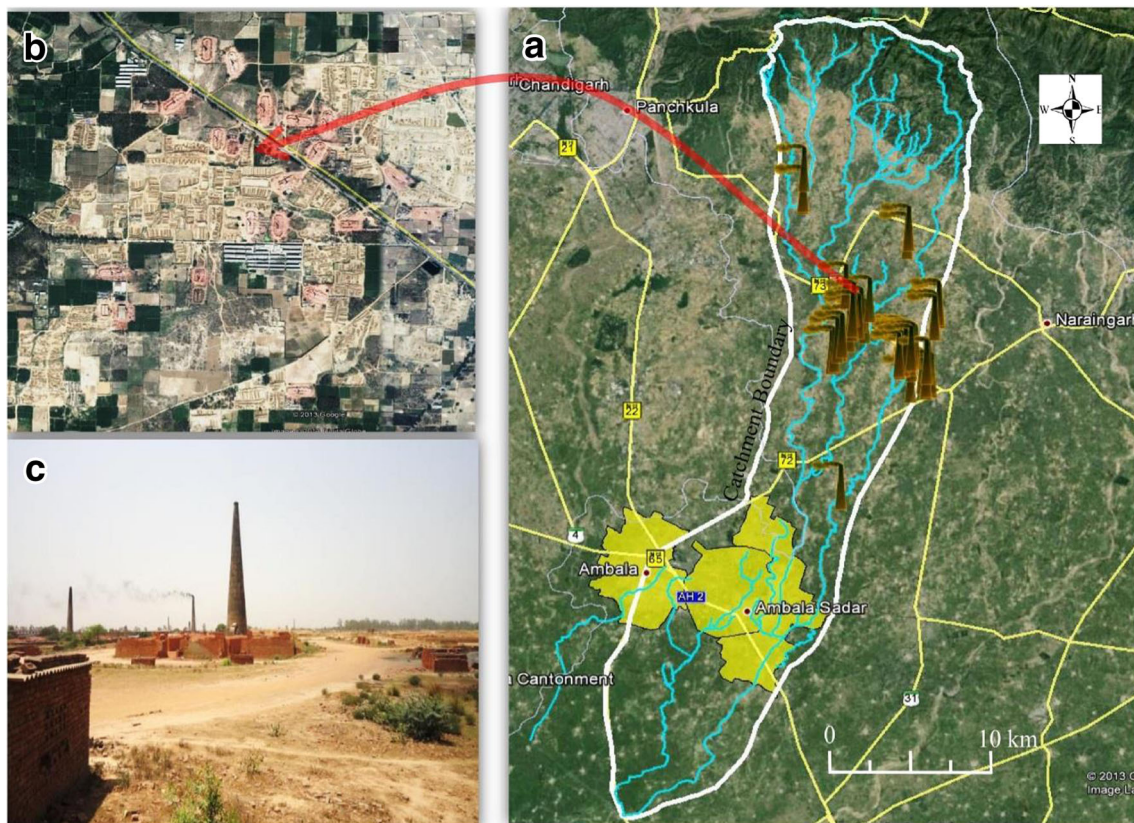


**Fig. 7** Google Earth (2012) image on regional scale (a). Enlarge view of Google Earth showing cluster of brick kiln industry (b). Field photo (2012) of the same location, located along NH-73 near village Kakarmajra (c). Source: field survey, 2012 and Google Earth (2012)



rivulets. Consequently, unconfined runoff moves in wide sheet of water causing sheet erosion, which further enhance the problem of siltation in Ambala urban area.

#### *Inadequate flood control structural measures*

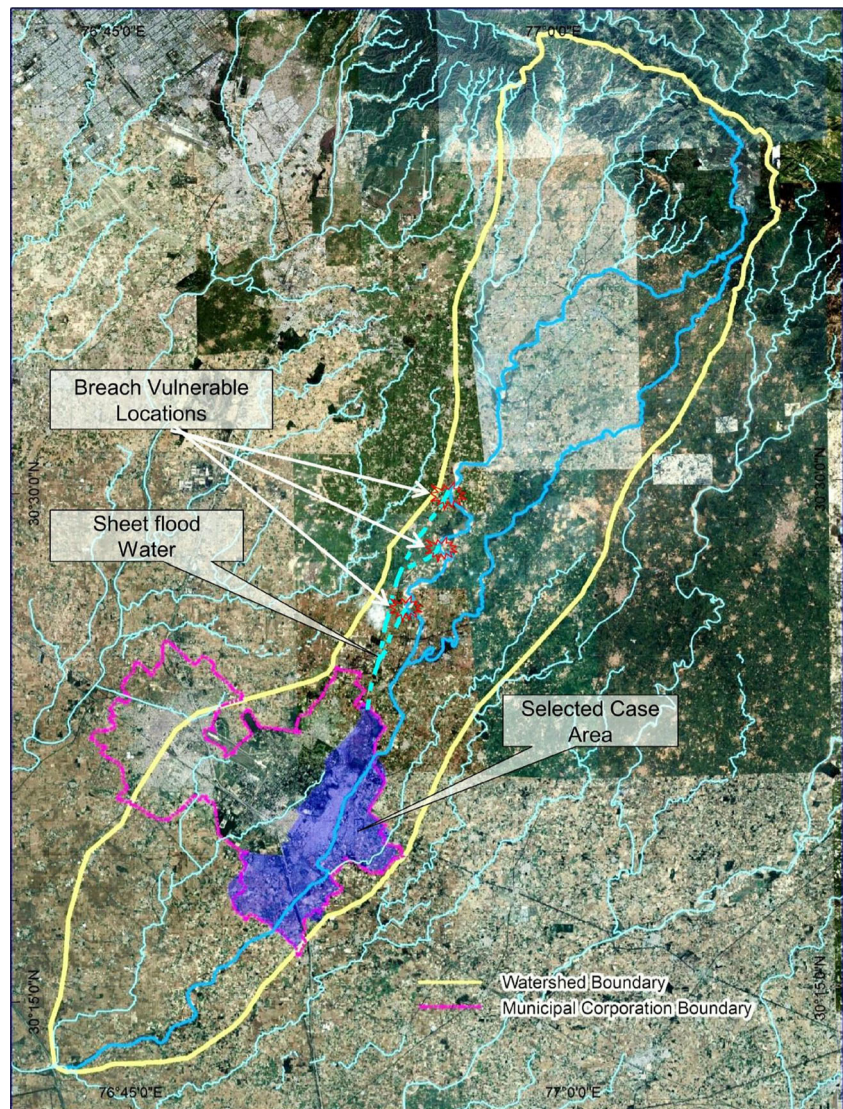
After the devastating flood of July 2010, Ambala district administration has taken up various protective and preventive measures to check the flood, particularly in the city and its outskirts. There is clay embankment on the right side while the river Tangri passes through the urban area (Ambala Disaster Management Action Plan 2012). However, beyond the city limit towards the upper catchment, flood protection measures are yet to be developed. Based on field observation and GIS analysis,

the research team found that due to the high gradient and shallow bed level of the Tangri River, flood water overflows the fragile banks mainly on the right side, as demonstrated in Fig. 8. This overtopping flood water forms sheet flood and enters the Ambala Sadar area from the village Boh and Cantonment side. Consequently, most and frequently affected localities are Dayal Bagh, Mahesh Nagar, Gobind Nagar, Kabir Nagar, Durga Nagar, and Ram Nagar, located on the right side of the main Tangri River.

#### *Expansion of impervious/built-up area*

Increasing urbanization adds to the surface runoff due to expansion of impermeable cover through the unplanned

**Fig. 8** Vulnerable breach location at River Tangri (field survey, 2012; Google Earth 2014)



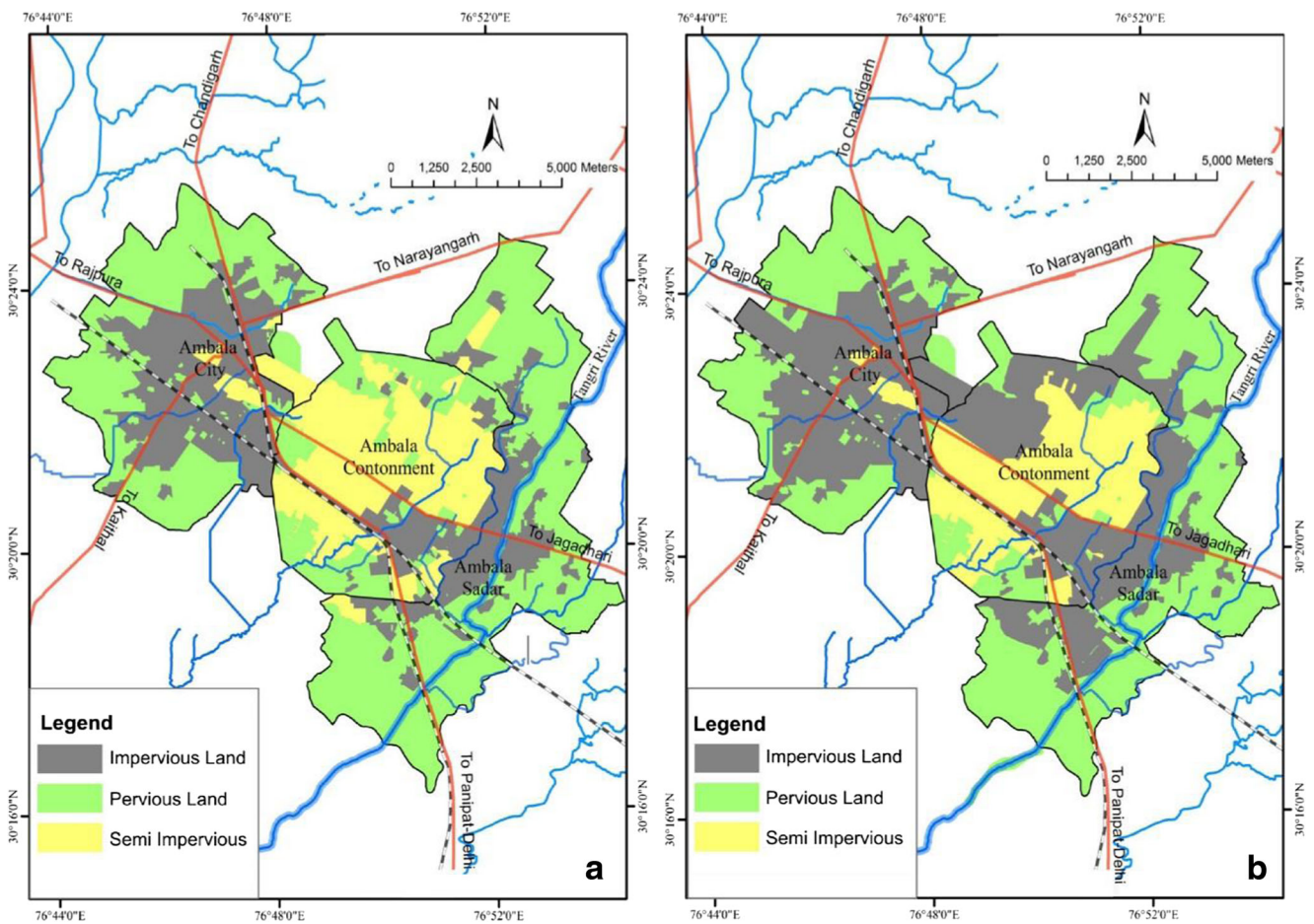


**Fig. 9** Urban built-up area growth during 2001 (a) and 2010 (b) within the Municipal Corporation boundary (Google Earth 2001, 2010)

construction of buildings, roads, pavements, and the like, which reduces infiltration and increase flood volume and peak as well (Johnson and Sayre 1973). This situation is more critical where sewage and drains are

under capacity. During the last two decades, the urban population has increased by 28 and 43 % between 1991 and 2001 and 2001 and 2011, respectively (Census of India 2011). The research team examined the satellite

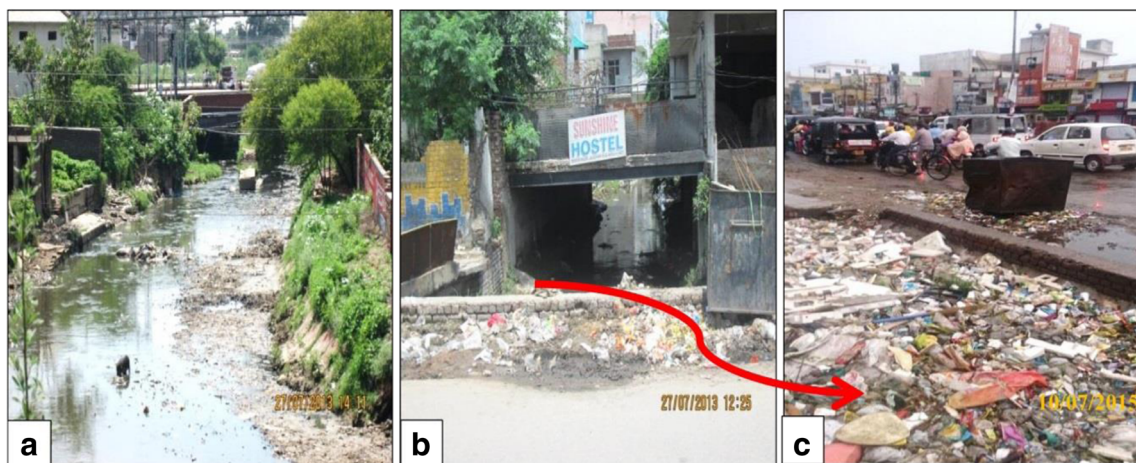


**Fig. 10** Open drains blocked by rubbish and garbage: Chaura Nala (local drain) crossing at NH-1 (a) and Mahesh Nagar drain (local drain) crossing at Jagadhari road (b, c) (field survey, July 2013 and July 2015)

imagery (1 m resolution) for the years 2001 and 2010 available on Google Earth; built-up area is extracted for both the periods using GIS, as presented in Fig. 9. The total impervious land (built-up/covered surface) have increased from 12 % in 2001 to 17 % in 2010 in the whole Tangri watershed, while at urban scale (Municipal Corporation), it increased from 35 to 47 % during the same period.

#### *Disposal of solid waste and under capacity drainage system*

There are four prominent local drains, including Ambala drain, Mahesh Nagar drain, Gudgudia Nala, and Chaura Nala (Fig. 10) to dispose waste water. These drains are blocked with residue released from the residential colonies. Cow dung thrown in the drains by milk dairies located in thickly populated residential areas choked sewerages and significantly reduced the natural flow of water. The problem of flooding is further intensified by the under capacity of the drainage system (Ambala District Disaster Management Plan (DDMP) 2015). Moreover, according to Ambala City DDP 2025, till year 2010, only 10 % of the city's area was covered with sewerage and there were no sewage treatment plant. Consequently, untreated sewage was discharged

into the storm/open drains, which caused an increase in impermeability and peak flow as well (Ambala City Draft Development Plan (DDP) 2025 2012).

#### *Land under natural drains is not a state property*

In general practice, land under natural drains/streams is state or government property. However, Haryana state has a unique problem, i.e., at many places, this land is private property and people have started constructing on it, causing not only obstruction to the natural flow of water but also putting the houses at flood risk (The Tribune 2007). Figure 11 presents an unplanned development/encroachment which starts from north tip to south tip along the main Tangri River in the Municipal Corporation jurisdiction. Consequently, natural infiltration has reduced and runoff response increases pressure on storm water drainage and damage downstream.

#### *Appraisal of Ambala City's Draft Development Plan—2025*

Ambala City's Draft Development Plan (DDP) 2025 explanation report and drawing bearing number *DTP (A) 2922/2012*, dated the *5th May 2012*, provided by the Town and Country Planning Department Haryana (2012), and this was reviewed from the point of view

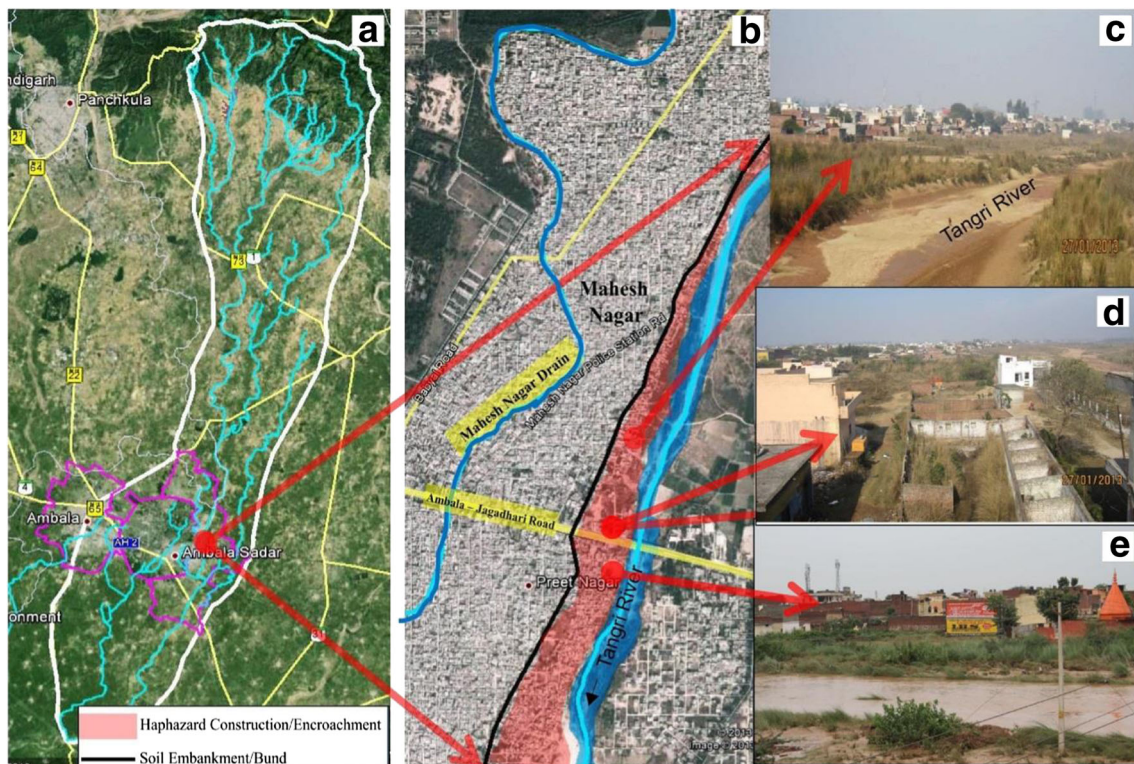


**Fig. 11** Google Earth (2012) image at regional scale (a), blowup portion on Google image, showing construction inside the River embankment (b), and field photographs (2013) of haphazard development inside the River embankment (c–e)

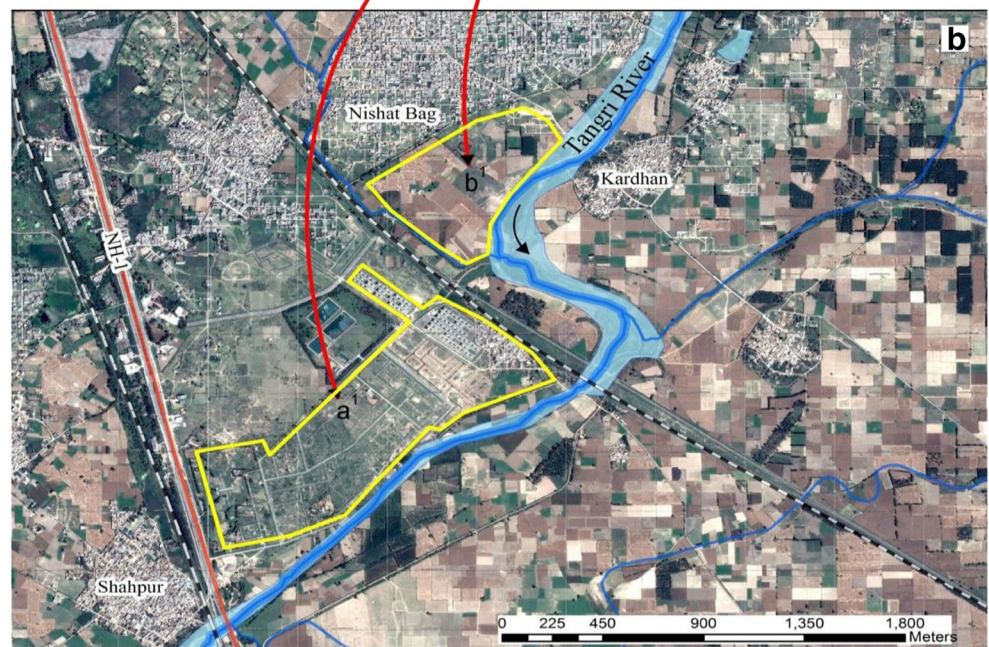
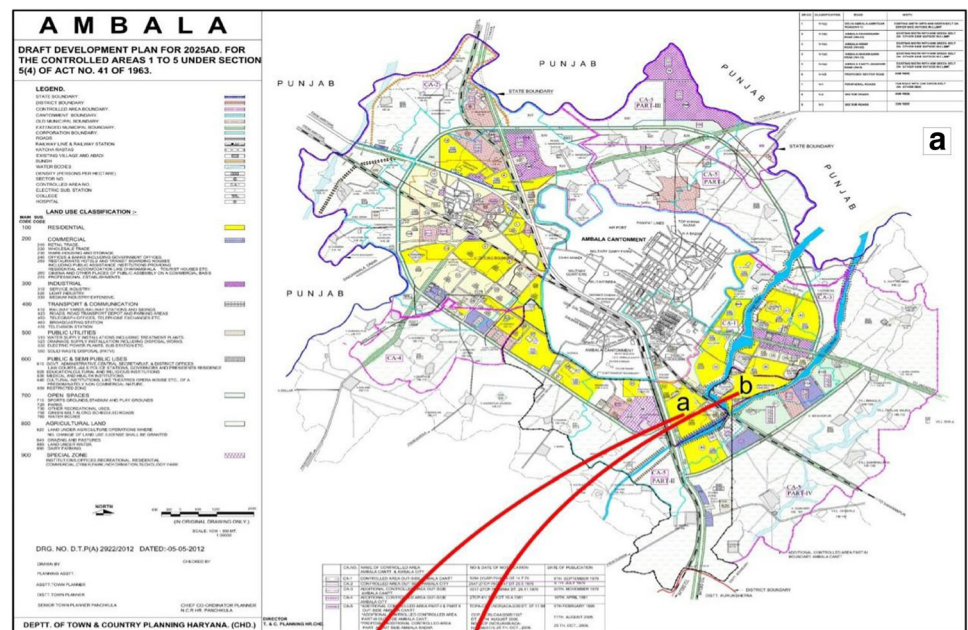
on whether or not the proposed development is consistent with flood-prone locations. Figure 12a represents a copy of the original, showing the development proposals as per DDP 2025, and in Fig. 12b (at points a1 and b1), a proposed residential development (yellow highlighted) is shown, and we examined that this site is not suitable for residential/built-up, because these locations are falling under the immediate floodplain of high-risk zone. Consequently, on account of the proposed built-up, it may increase runoff and damage also. Instead, at these locations, development proposal should be pervious in

nature, like playground or agriculture to ensure that flood risk is reduced to acceptable levels. After the appraisal of DDP 2025, the research team revealed that DDP 2025 does not demarcate flood plain zoning and also does not perceive long-term flood risk at danger level.

### Flood-risk modeling in selected area

Based on flood history and impact, Ambala Sadar area (Fig. 13) was found to be critically flood affected within

**Fig. 12** a Locations of non-compatible land use in draft development plan—2025 (Town and Country Planning Department Haryana 2012). b Google Earth (2013) image shows the corresponding locations highlighted with yellow polygons



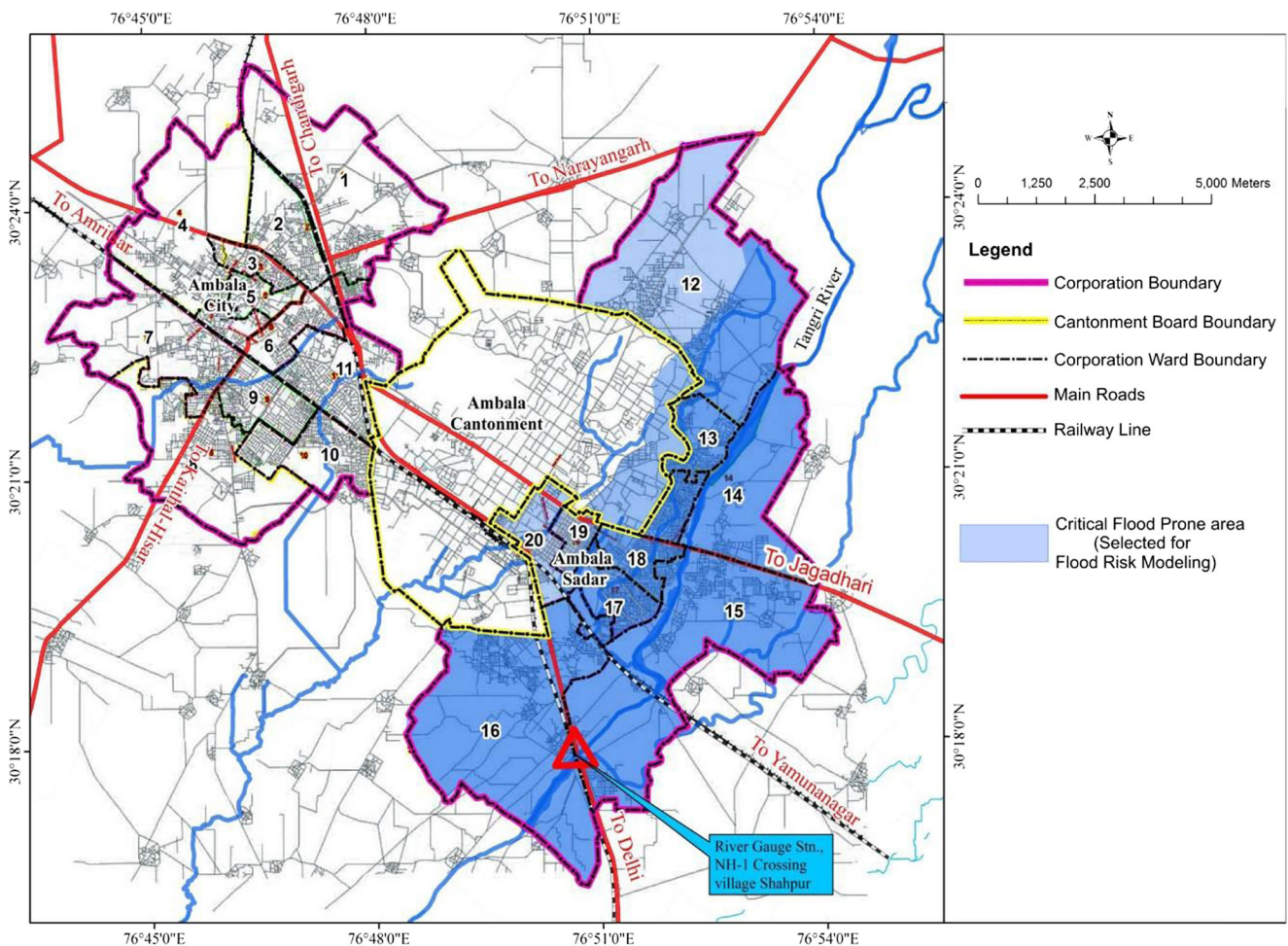


**Fig. 13** Location of critical flood-prone area

the Ambala Municipal Corporation (Ambala District Disaster Management Plan (DDMP) 2015). Therefore, it was selected for detailed analysis and flood inundation modeling according to different probabilities of flood. The existing river gauge station, located at NH-1 crossing near village Shahpur, is considered a watershed outlet. At this location, we measured 516 km<sup>2</sup> of watershed. The selected case area comprised 56.25 km<sup>2</sup> with a total population of 182,577, which constitutes about 40 % of the total population of Ambala Municipal Corporation and distributed in nine wards (ward nos. 12–20), as listed in Table 2

**Flood frequency calculation using observed peak flow data**

There are several formulas available in literature for flood probability analysis using observed maximum flow data and providing different results. Among them, *Weibull's plotting position* formula is most popular, particularly for rainfall/flood frequency studies (Adamowski 1981; Subramanya

2013). This formula is expressed as  $T = 1/P = (n + 1)/m$ , where  $T$  is recurrence interval in years,  $P$  is probability of an exceedances in any 1 year,  $n$  is the number of the years of the record, and  $m$  is the descending order number of magnitude

**Table 2** Critical flood zone: area and population (Census of India 2011)

Ward no.	Area (ha)	Population	Population (%)	Density (persons/ha)
12	1313.24	14,140	7.74	11
13	167.66	22,779	12.48	136
14	737.38	19,082	10.45	26
15	1359.6	30,724	16.83	23
16	1375.13	16,929	9.27	12
17	170.9	12,216	6.69	71
18	148.9	17,932	9.82	120
19	91.93	28,643	15.69	312
20	260.26	20,132	11.03	77
Total	5625	182,577	100.00	32

(Subramanya 2013). In the present study, Weibull’s plotting position method is used for flood frequency calculation. The observed annual maximum flow data (m<sup>3</sup>/s) covering 21 years (1990–2010) for NH-1 station, near village Shahpur were obtained from the Executive Engineer of Water Data Collection Division, Karnal, Government of Haryana. Based on flood history data, the research team found that the study area is frequently affected by flooding, therefore, a 20-year return period is considered longest return period for the flood-hazard zone delineation. Table 3 and Fig. 14 present the probability in terms of different magnitudes and their chance of recurrence in percent and return period. These calculated peak flow frequencies are 663, 1032, 1127, and 1238 m<sup>3</sup>/s against 2-, 5-, 11-, and 22-year return periods, respectively. However, for the sake of convenient inundation modeling and rounding the discharge value to the nearest hundred, excluding 2-year return period, we have considered assumed peak flows such as 663, 1000, 1100, and 1200 m<sup>3</sup> for 2, 5, 10, and 20 years, respectively. Though, if we refer to Table 3, these assumed peak flows corresponding to respective return periods were found about 3–4 % less than the calculated values. Table 4

**Table 3** Flood frequency analysis based on maximum flows recorded at the river Tangri near village Shahpur, Water Data Collection Division, Karnal, Government of Haryana, 2014)

Year (n = 21)	Maximum flow Q (m <sup>3</sup> /s) in descending order	Rank (m)	Probability P (in %)	Return period (T; 1/P; year)
1995	1238	1	4.5	22.0
2010	1127	2	9.1	11.0
2004	1081	3	13.6	7.3
2002	1032	4	18.2	5.5
2008	994	5	22.7	4.4
1997	954	6	27.3	3.7
1996	919	7	31.8	3.1
1994	918	8	36.4	2.8
1993	917	9	40.9	2.4
2009	866	10	45.5	2.2
2005	663	11	50.0	2.0
1992	602	12	54.5	1.8
1990	574	13	59.1	1.7
2003	540	14	63.6	1.6
2000	452	15	68.2	1.5
2001	394	16	72.7	1.4
2007	373	17	77.3	1.3
1999	321	18	81.8	1.2
1998	255	19	86.4	1.2
1991	35	20	90.9	1.1
2006	27	21	95.5	1.0

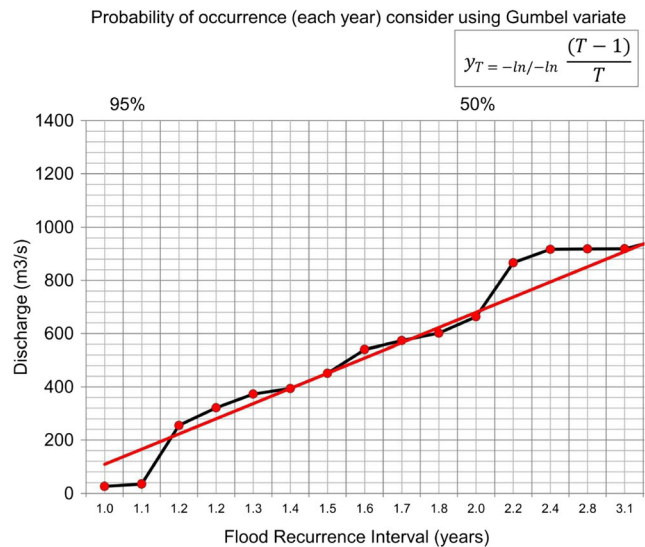


**Fig. 14** Flood-frequency curve

represents the assumed peak discharge and their probability of occurrence (%) against the respective return periods.

**Data requirements for flood inundation modeling**

In order to perform flood scenario modeling against different magnitude probability, the analytical procedure presented in Fig. 15 was followed in GIS environment. The essential geometric data layers shown in Fig. 16 were developed in a GIS framework by referring to HEC-RAS user’s manual (USACE 2002).

*Digital elevation model*

It is the mandatory input for the flood modeling; hence, Cartosat-1 DEM (30 m) is used in this study (National Remote Sensing Centre Hyderabad 2013).

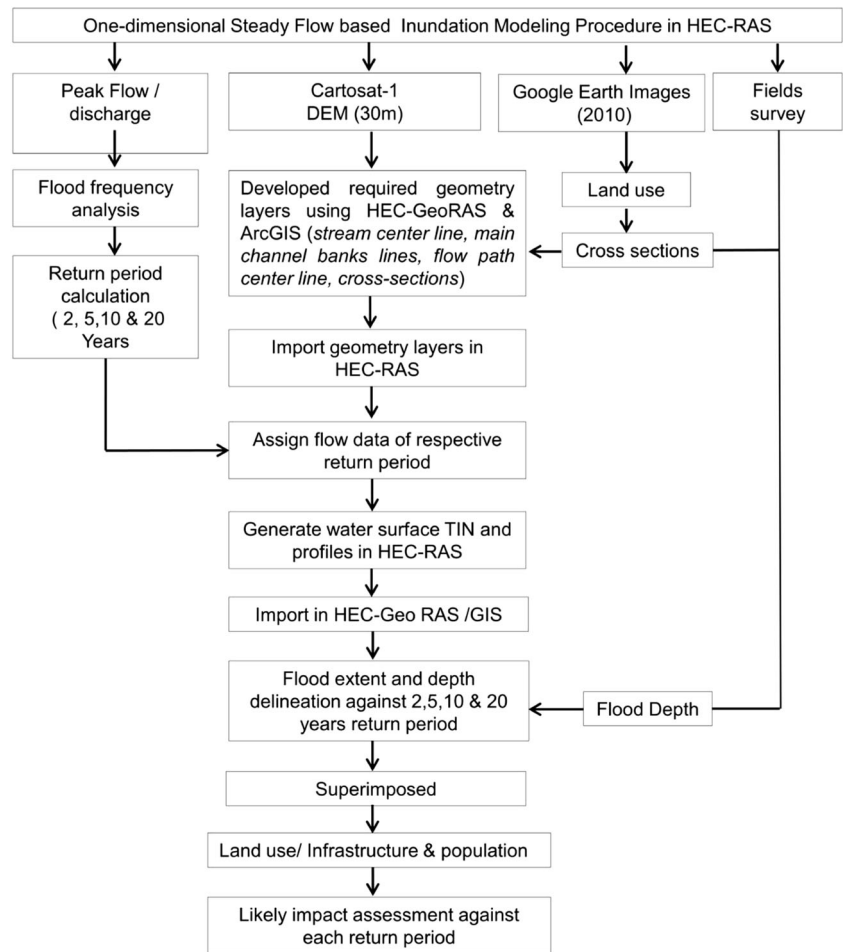
*Main stream centerline*

It is produced based on processed DEM and corrected with reference to Google Earth (2010).

**Table 4** Assumed flood frequency considered for inundation modeling

Return period (years)	Peak discharge (m <sup>3</sup> /s)	Probability of recurrence
2	663	50 % chance/2 years
5	1000	20 % chance/5 years
10	1100	10 % chance/10 years
20	1200	4 % chance/20 years

**Fig. 15** Analytical procedure for flood inundation modeling in HEC-RAS software



*Main channel banks line*

Both left- and right-side banks are required to separate the below and overbank area so that bank lines are digitized using topographic maps and Google Earth (2010).

*Flow path centerline*

As per rule of thumb, it is generally created towards the direction of flow and is required to assess hydraulic flow (USACE 2002)

*Cross-section 3D cut lines*

To represent the change in slope, shape, roughness, structure of the main channel, and adjoining floodplain, these cross-sections are drawn based on DEM. Cross-sections were

depicted from left to right while looking downstream (HEC-RAS v4.1 User Manual 2010).

*Boundary conditions*

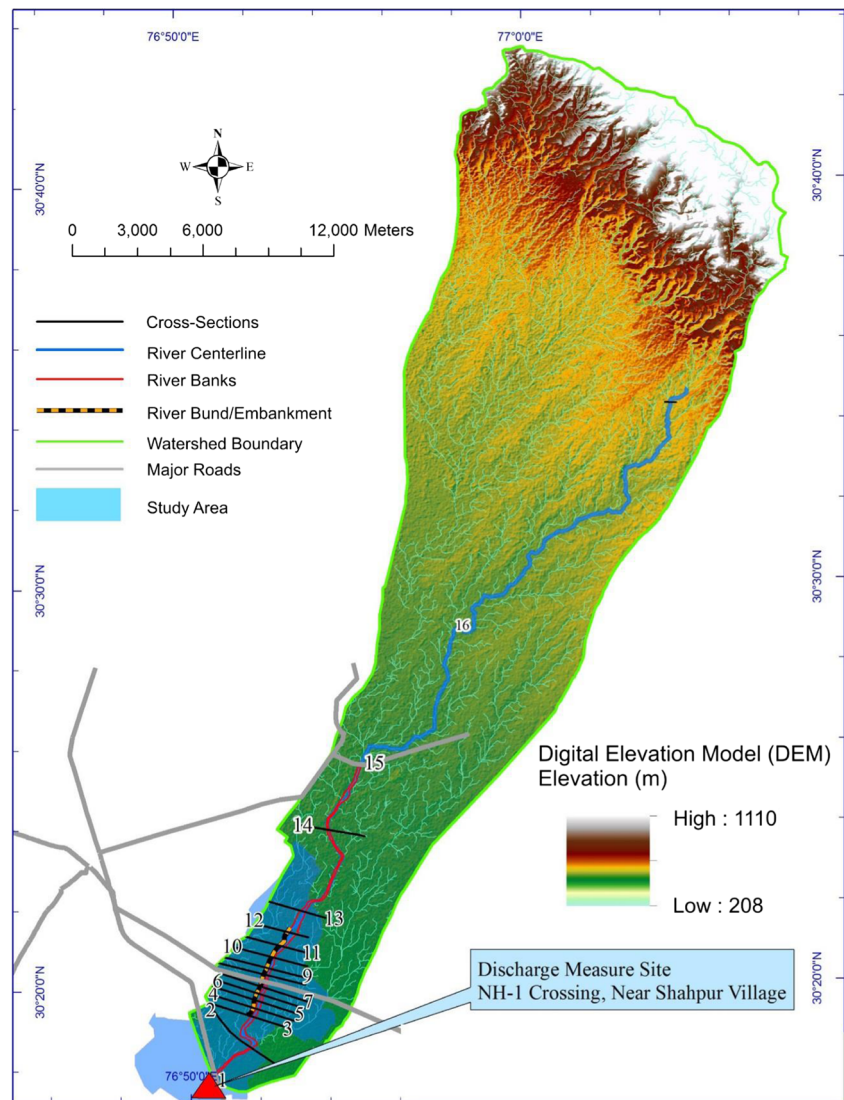
These include the slope and critical depth (USACE 2002).

*Selection of Manning roughness coefficients (or Manning's n)*

The Manning's *n* is a coefficient which represents the roughness or friction to the flow in open channel and flood plains (Chow 1959). Manning's *n* can be evaluated by cross-sections demarcated over channel or floodplain of a longitudinal reach. Manning's *n* equation is an empirical equation (Chow 1959) and is generally written as:

$$V = \frac{1}{n} R^{2/3} S_e^{1/2} \tag{1}$$

**Fig. 16** Geometric data layers backed with Cartosat-1 (30 m) DEM (National Remote Sensing Centre Hyderabad 2013)



Where:

- $V$  Mean velocity of flow (m/s)
- $R$  Hydraulic radius (m)
- $S_e$  Slope of energy grade line (m/m)
- $n$  Manning's roughness coefficient

The roughness coefficient ( $n$  values) within channel or floodplain is affected by several factors, such as shape and size of channel, composition of bed by material type and size, vegetation type and growth, velocity/ stage of flow in channel, and irregularity of surface in floodplain. As a result, Manning's  $n$  varies over time and space in open/constructed channels and floodplains (Ree 1954; Chow 1959; Carter et al. 1963; Barnes 1967). Normally, floodplain roughness is higher than the channel roughness (Chow 1959). On account of these

above-mentioned factors, Manning's  $n$  cannot be specified with desirable accuracy by direct measurement of roughness. Therefore, Manning's  $n$  must be tuned against flooding data, and  $n$  values should be determined separately for floodplains and channels (Cowan 1956). The relative accuracy of  $n$  values can be improved by using field photographs and having field experience (Barnes 1967). Based on the outcomes of the literature review, we have adopted the recommended Manning's  $n$  values for channel and flood plains from the reference table found in Chow (1959). For urban, which includes built-up area under residential, commercial, public semipublic, and industrial, the  $n$  values assigned were 0.1, with the assumptions that there could be large resistance in the flow (Syme 2008). Focusing on the case area, we have delineated 14 cross-sections of irregular interval over Cartosat-1 DEM (30 m).



These cross-sections were drawn perpendicular to the flow line (USACE 2002), extending to the focused area limit. In order to produce qualitative inundation output, high-resolution topographic data plays a significant role (Mason et al. 2003). Therefore, due to the poor resolution of Cartosat-1 DEM (30 m), the research team conducted field surveys especially for measuring topographic elevation ( $z$ ) and channel depth using handheld GPS and scaled vertical iron rod. The main channel of the River Tangri is found mostly straight with shallow and sandy bed. Since the roughness varies across the width of the cross-section, a large-scale (parcel level) land use/land cover map derived from Google Earth (2010) images was incorporated to determine the base  $n$  value corresponding to each subdivision intersecting the portion of different types of land use (Fig. 17). The land use types un-

derlying the respective cross-section were related to the corresponding base  $n$  values from the table of Chow (1959). This approach was later contradicted by Straatsma and Baptist (2008); they point out that land use changes over time and space, so  $n$  values do not coincide with actual physical condition, and they have suggested that roughness values should be compatible to ground condition to reduce variation of input parameters during calibration. However, several studies estimated Manning’s  $n$  at reasonable accuracy based on a lookup table of land use/land cover applied to hydrodynamic-numerical models (Brun and Band 2000; Hossain et al. 2009; Lumbroso and Gaume 2012). In order to determine and improve the accuracy of  $n$  values of channel and flood plain, the research team has used high-resolution Google Earth (2013) images and field photographs (Fig. 18), and the

**Fig. 17** Assigned roughness coefficients (adopted from Chow 1959) to channel and floodplain based on land use/land cover (Google Earth 2010)

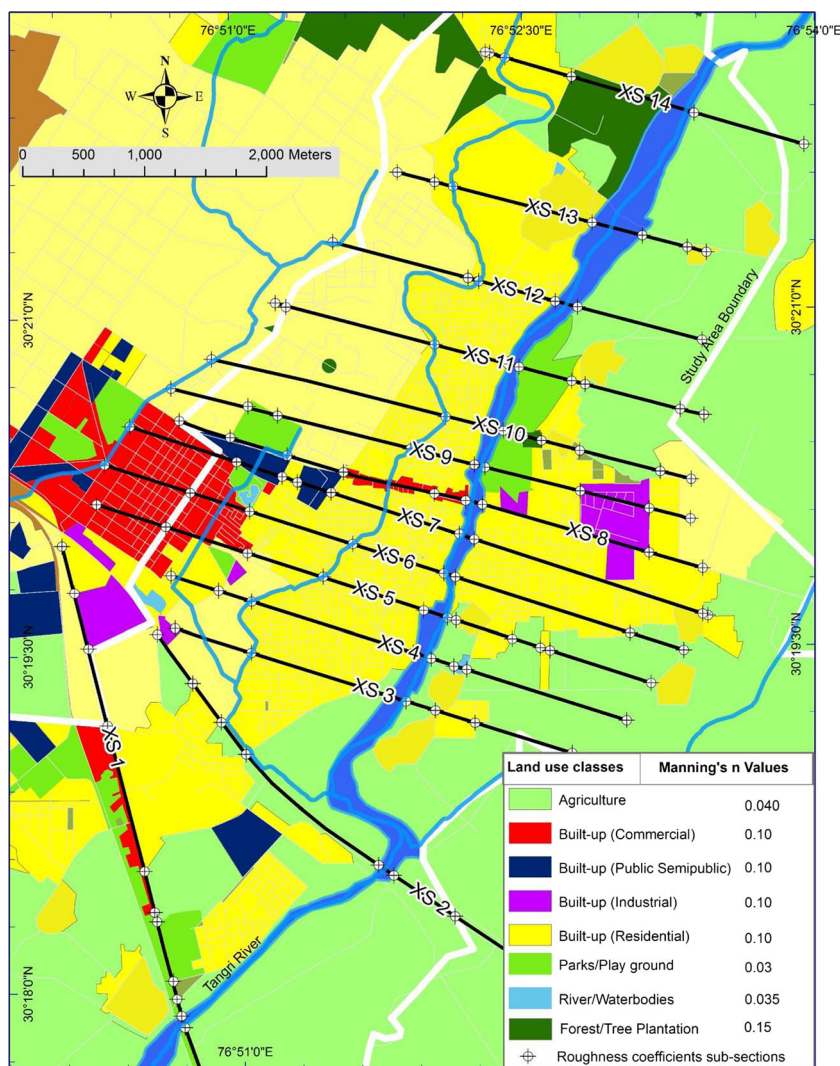
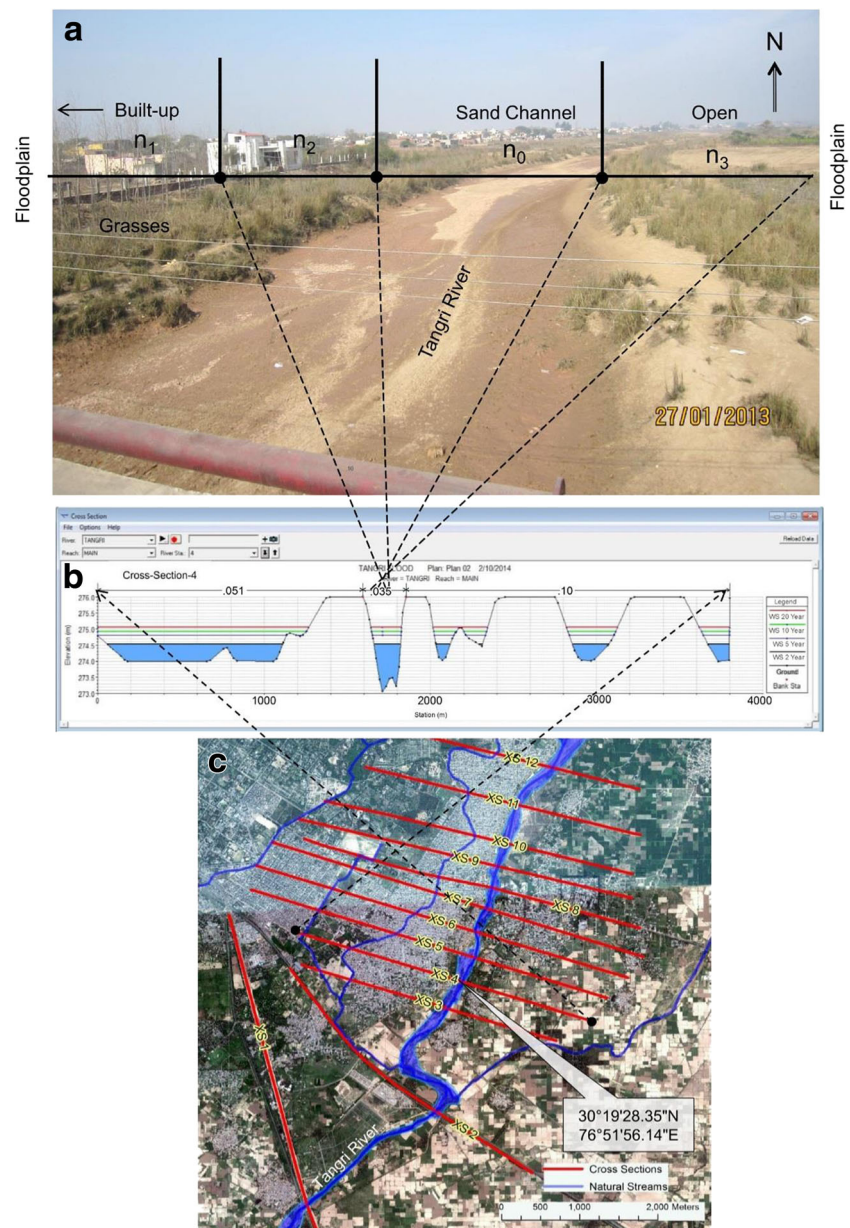


**Fig. 18** Adjustment of  $n$  value for channel and flood plain by relating the table modified from Aldridge and Garrett (1973) and verification photograph (2013) (a). Steady flow water surface profile corresponding to cross-section 4 (b). Cross-sections overlaid on Google Earth image to assist in determining roughness coefficients in channel and floodplain (c)



adjustment values (Table 5) for factors affecting the roughness for channel adopted from Cowan (1956), and for floodplain, adjusted  $n$  values were adopted from the table modified from Aldridge and Garrett (1973). The adjusted  $n$  values which appeared in parentheses (Table 5) were taken after the addition of the base  $n$  value (Chow 1959) and factor adjustment  $n$  value (Cowan 1956; Aldridge and Garrett 1973) for each subdivision (from  $n_0$  to  $n_2$ ) of the corresponding cross-section. Thus, based on channel and over bank floodplain condition, Table 5 reveals that the adjusted  $n$  values vary between 0.005 (channel portion) and 0.011 (left over bank).

### Performing one-dimensional steady flow analysis using observed peak flow data

According to HEC-RAS v4.1 User Manual (2010), “steady flow is a condition in which depth and velocity at a given channel location do not change with time. Gradually, varied flow is characterized by minor changes in water depth and velocity from cross-section to cross-section.” Tate (1999) explained in the HEC-RAS manual that “the basic computational procedure of steady-flow surface profiles is based on an iterative procedure also called the standard step method.

**Table 5** Adjustment of base  $n$  values from Chow (1959) for factors that affect the roughness of flood plains (adopted from the table modified from Aldridge and Garrett 1973)

Cross-section number	Base $n_1$ (ROB)	Adjusted $n_1$ values (ROB)	Base $n_0$ (channel)	Adjusted $n_0$ values (channel)	Base $n_2$ (LOB)	Adjusted $n_2$ values (LOB)
14	0.045	(0.045)	0.035	0.000 (0.035)	0.040	0.011 (0.051)
13	0.10	(0.10)	0.035	0.005 (0.040)	0.040	0.011 (0.051)
12	0.10	(0.10)	0.035	0.005 (0.040)	0.040	0.011 (0.051)
11	0.10	(0.10)	0.035	0.005 (0.040)	0.040	0.011 (0.051)
10	0.10	(0.10)	0.035	0.005 (0.040)	0.100	0.100 (0.100)
9	0.10	(0.10)	0.035	0.005 (0.040)	0.100	0.100 (0.100)
8	0.13	(0.13)	0.035	0.005 (0.040)	0.130	0.130 (0.130)
7	0.10	(0.10)	0.035	0.005 (0.040)	0.100	0.100 (0.100)
6	0.10	(0.10)	0.035	0.005 (0.040)	0.100	0.100 (0.100)
5	0.10	(0.10)	0.035	0.005 (0.040)	0.100	0.100 (0.100)
4	0.10	(0.10)	0.035	0.005 (0.040)	0.040	0.011 (0.051)
3	0.10	(0.10)	0.035	0.005 (0.040)	0.040	0.011 (0.051)
2	0.13	(0.13)	0.035	0.005 (0.040)	0.130	0.130 (0.130)
1	0.13	(0.13)	0.035	0.005 (0.040)	0.130	0.130 (0.130)

$n$  values after adjustment (base  $n$  value + adjustment  $n$  values) are enclosed in parentheses

$n_0$ – $n_2$  subdivision of cross-sections, *ROB* right over bank floodplain, *LOB* left over bank floodplain

In order to execute the inundation model and to generate water surface elevation profiles from peak flows corresponding to 2-, 5-, 10-, and 20-year return period flood, we have assigned the adjusted  $n$  values (given in parentheses) with reference to Table 5. Finally, the predicted peak flow of a respective return period was conveyed through each cross-section using HEC-RAS procedure. Figure 19, as an example, presents the water surface elevation profile against cross-section numbers 12, 4, and 3.

## Result and discussion

### Likely impact by flood extent

HEC-RAS flood modeling result revealed that the area at risk to flooding will be 932, 1511, 2031, and 3147 ha, corresponding to 2-, 5-, 10-, and 20-year return flood, respectively, and with reference to 2-year flood, the increased flooded area are 62 % (5 years), 118 % (10 years), and 238 % (20 years), respectively. In order to perform ward-wise impact analysis, the modeled flood extent layer of each return period were intersected with the ward boundary (Fig. 20).

### Likely impact by flood depth

In order to generate flood depth map, the research team interviewed the local people with respect to flood history and respective water levels. Based on the ground information, we have found that the study area has experienced an average of 3–4 ft of flood depth with 4–5 days duration during all past flood events everywhere. For the most recent flood which occurred during 6th–8th July 2010, the research team conducted site survey during post-flooding period (9th–10th July 2010) in flood-affected localities. Flood level samples were collected through interviews from selected local flood-affected residents, and flood water mark/clue on various structures were identified and marked on hardcopy map. The collected flood water depth level samples were then digitized in point vector layer, and flood depth values were attached an attribute in GIS environment. To know the flood depth of non-surveyed areas, the depth points were interpolated using natural neighbor method in GIS environment. Finally, flood depth map shown in Fig. 21 was superimposed on the flood extent map in order to calculate area under each water depth category (Table 6). With reference to literature available on past flooding scenarios (Ahlawat and Bansal 2010), an average of 2–3 ft of flood depth is considered against all

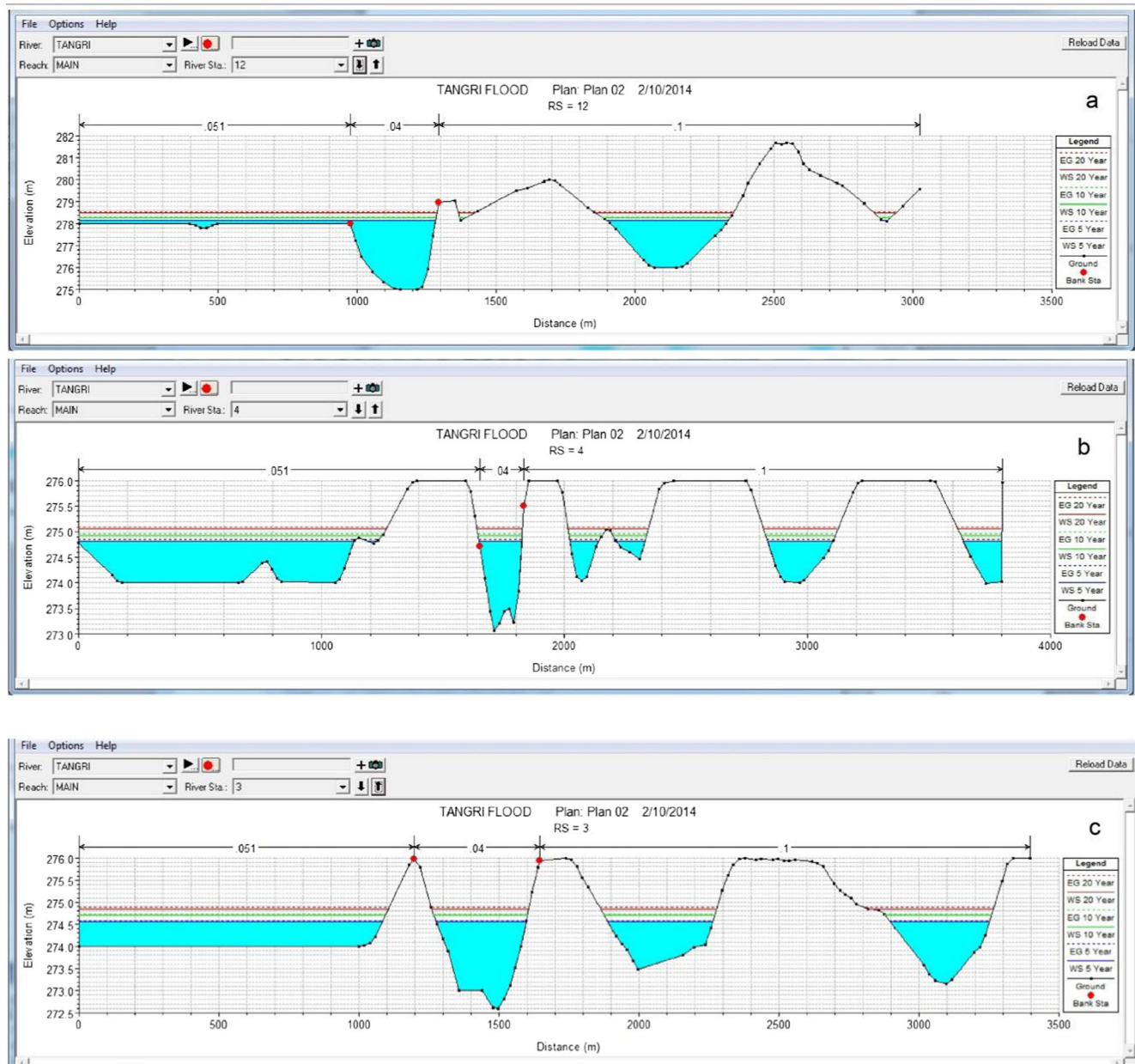


**Fig. 19** An example of HEC-RAS generated water surface profile corresponding to 5-, 10-, and 20-year return flood at cross-section 12 (a), cross-section 4 (b), and cross-section 3 (c)

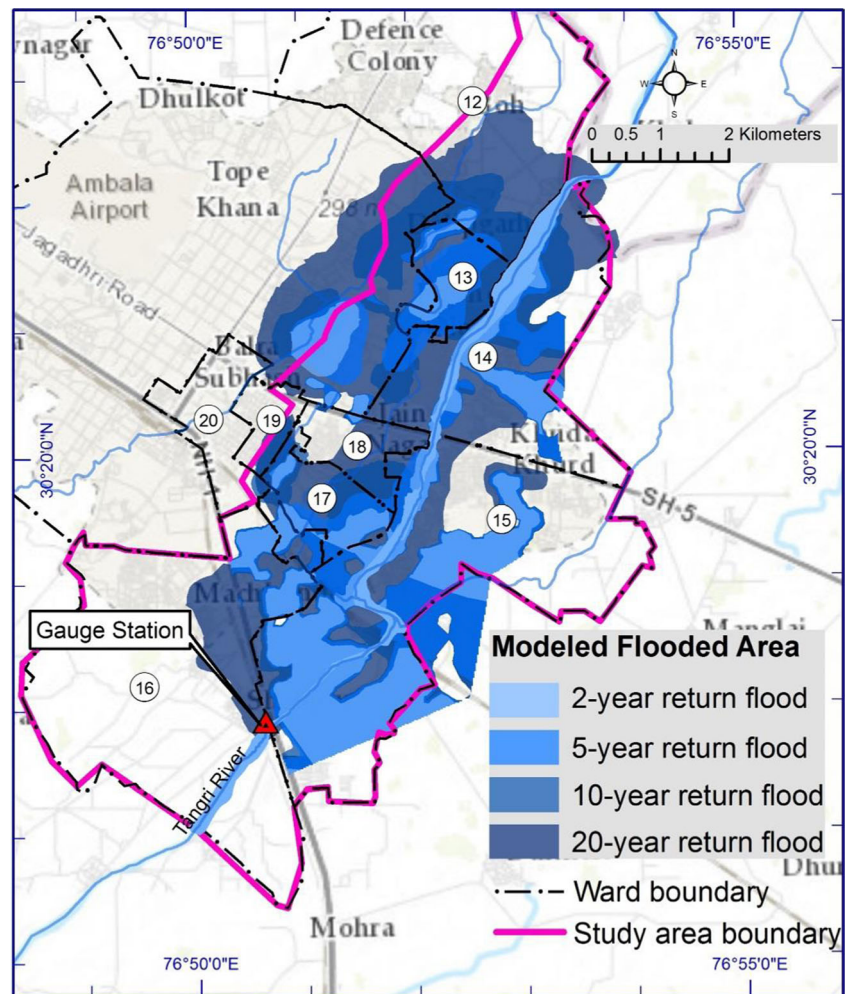
return period for the estimation of likely flood impact by depth.

### Likely impact on land use

Table 7 and Fig. 22 show the likely affected area under different land uses according to different flood probability. However, maximum likely flood affected area (about 65 %) against each return flood comes under open/green space

(parks, agriculture, water bodies, etc.), and these land usages are pervious in nature, so economic loss will not be so significant. On the other side, in terms of potential damage/economic loss, from the built-up area, the largest vulnerable land uses are residential, followed by commercial (market, shops), public and semipublic (educational, health, and utility services), roads/transportation, and industrial. Flooded area is estimated at 221 ha (4 %), 362 ha (6.5 %), 645 ha (11.5 %), and 971 ha (17 %) of total built-up area for a 2-, 5-, 10-, and

**Fig. 20** Modeled flooded extent corresponding to different return year flood



20-year return flood, respectively. To assess the ward-wise land use vulnerability, the modeled flood extent boundary layers (shown in hatching) were superimposed on existing land use layer/map and ward layer in GIS environment, as shown in Fig. 22. The large percentage of the total affected area comes under residential use from ward nos. 13 and 17 and ward no. 18 against each return period. These are low-lying localities and have most critical flooding situation. In terms of potential economic loss, ward nos. 18 and 19 are the most affected due to largest concentration of lifeline infrastructure including main roads (Jagadhari and Babyal road), schools, colleges, hospitals, shopping/commercial zone, and Sadar bazar.

### Likely impact on population

In terms of disrupting normal life during flooding in the study area, we have estimated the human population likely to affect

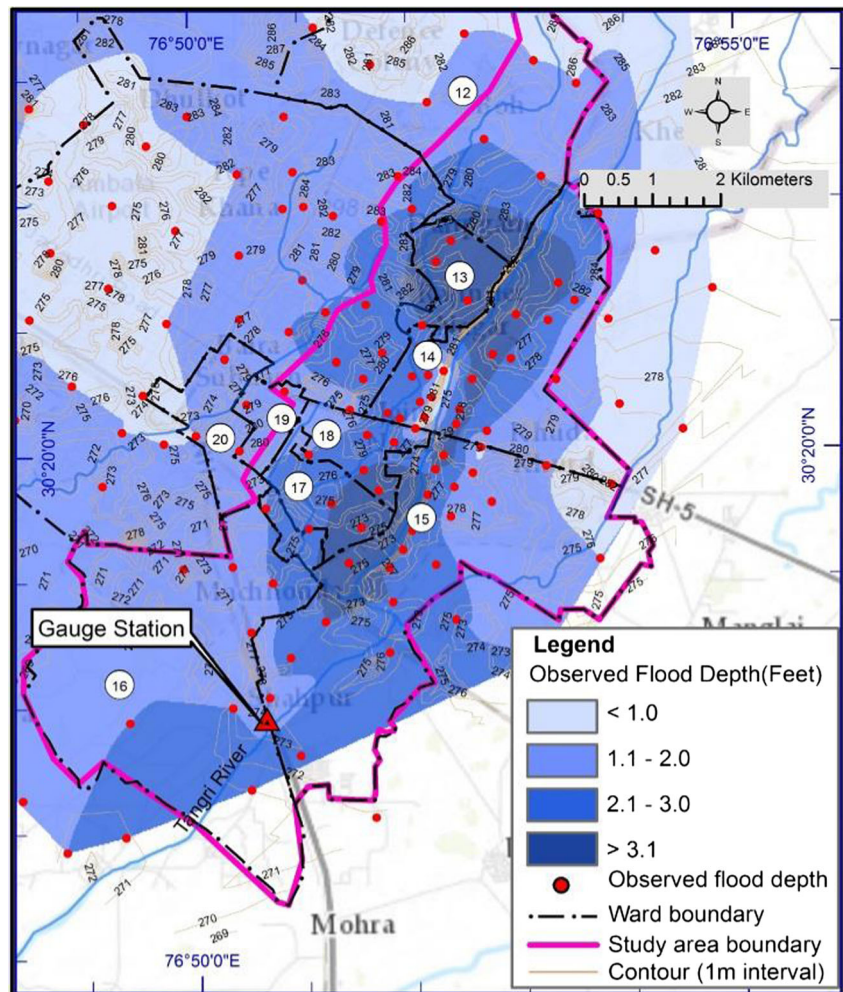
against longest flooding scenario of a 20-year return period. The affected population was derived by intersecting the 20-year flooded layer and ward boundary layer tagged with population data (Census of India 2011) in Arc GIS. It is found that the most populated wards are 13 and 19, followed by wards 18, 15, 17, and 14 (Table 8). Thus, intensity of flood impact on population will be in accordance. Since these estimates are based on current population density multiplied by modeled 20-year flood spread, hence, this figure may change if future projected population is considered.

### Validation of modeling results

*Validation of flood extent using remote sensing data and filed photographs*

The flood extent against 10-year return period was validated because the routed peak discharge was well

**Fig. 21** Flood depth estimation by interpolating the observed data of flood event—2010



matched with the observed flow, available for the latest flood event which occurred during 6–9 July 2010. On the other hand, during field surveys, flood elevation high-water marks/clues were identified (Fig. 23) and local newspaper clippings of flooding period and interview of local people were incorporated for validation of

flooding extent. In addition, remote sensing imagery of TM Landsat-5 (30 m), acquired on 15th July 2010 (Fig. 24) was used for the same flood period. Water remained for 3 days from 6th to 8th July 2010, but satellite imagery during peak flood was not available. Moreover, due to cloud cover, flooding water in high-

**Table 6** Likely flood depth according to flood frequency

Water depth (ft)	2 year flood area (ha)	5 year flood area (ha)	10 year flood area (ha)	20 year flood area (ha)
<1	45	60	70	200
1.1–2	90	125	180	300
2.1–3	338	550	650	1100
>3	217	400	630	700
Total flooded	690	1135	1530	2300
No flooding	4935.67	4490.67	4095.67	3325.67
Total area	5625.67	5625.67	5625.67	5625.67

**Table 7** Description of land use vulnerability against flood probability

Land use categories		2-year flood		5-year flood		10-year flood		20-year flood	
		Area		Area		Area		Area	
		ha	Percent	ha	Percent	ha	Percent	ha	Percent
Residential	Built-up	193.10	3.43	327.00	5.81	562.20	9.99	825.00	14.66
Commercial		7.50	0.13	11.50	0.20	38.00	0.68	61.00	1.08
Industrial		0.00	0.00	0.00	0.00	2.00	0.04	11.00	0.20
Roads/street		3.83	0.07	6.50	0.12	23.00	0.41	49.00	0.87
Public and semipublic		17.00	0.30	17.00	0.30	20.00	0.36	25.00	0.44
Park/play ground	Non-built-up	2.00	0.04	2.00	0.04	2.00	0.04	4.00	0.07
Open		289.07	5.14	593.50	10.55	705.30	12.54	1143.50	20.33
Water bodies		164.50	2.92	164.50	2.92	164.50	2.92	168.50	3.00
Slum		13.00	0.23	13.00	0.23	13.00	0.23	13.00	0.23
Flooded		690.00	12.27	1135.00	20.18	1530.00	27.20	2300.00	40.88
Non-flooded		4935.67	87.73	4490.67	79.82	4095.67	72.80	3325.67	59.12
Total area		5625.67	100.00	5625.67	100.00	5625.67	100.00	5625.67	100.00

dense built-up area was not interpretable. From 9th July onwards, the water level started receding and flood

adjacent to the study area was in good agreement against Fig. 23; this shows field photo of inundation and

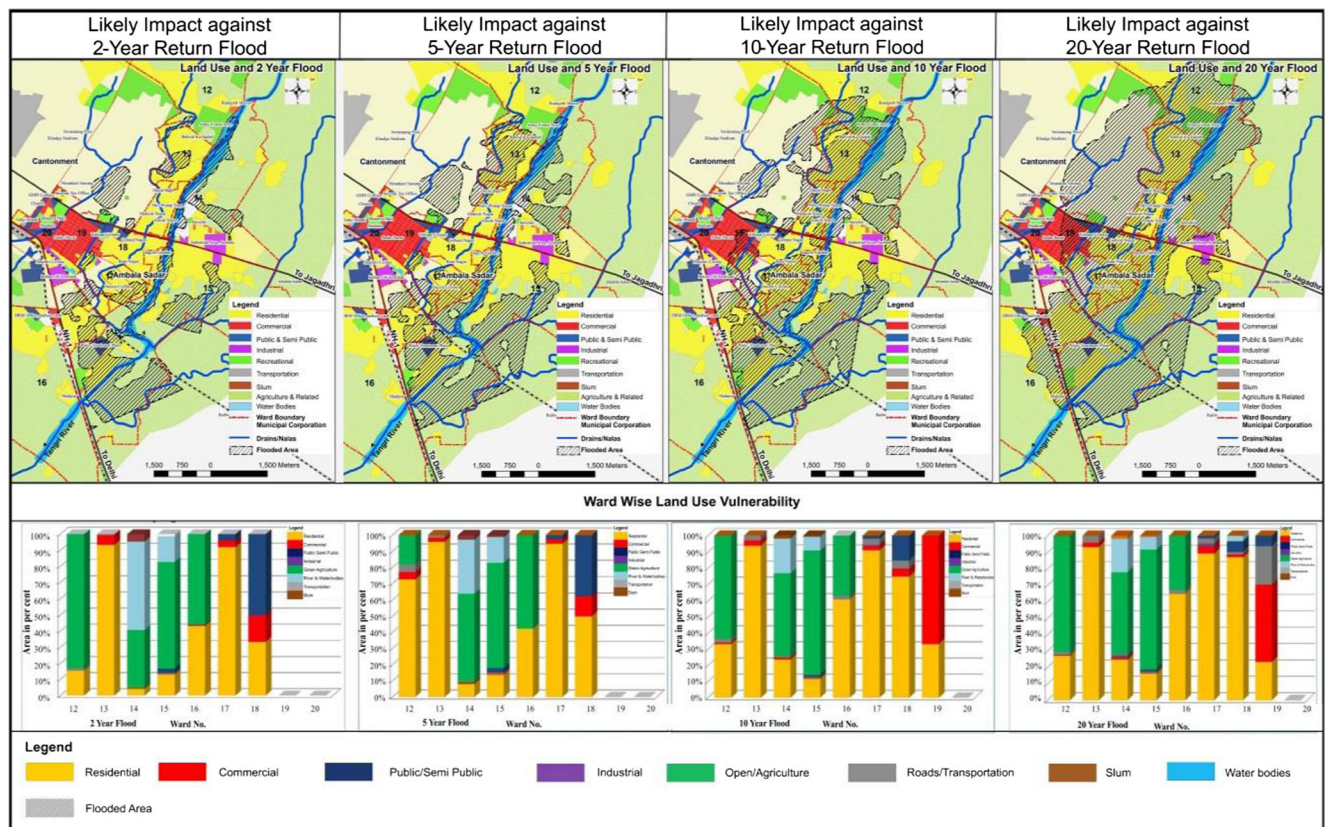


**Fig. 22** Ward-wise simulated flood impact on land uses according to different return periods

**Table 8** Ward wise likely affected area and population against 20-year flood scenario

Ward no	Area (ha)	Affected area (ha)	Affected area (%)	Population	Affected population	Affected population (%)	Density persons/ha
12	1364.61	256.00	18.76	14,140	2756	19	11
13	167.66	165.00	98.41	22,779	22,418	98	136
14	737.38	420.50	57.03	19,082	10,882	57	26
15	1359.60	1092.00	80.32	30,724	24,677	80	23
16	1375.13	92.00	6.69	16,929	1133	7	12
17	170.90	134.00	78.41	12,216	9578	78	71
18	148.90	126.00	84.62	17,932	15,174	85	120
19	91.93	85.00	92.46	28,643	26,484	92	312
20	260.26	0.00	0.00	20,132	0	0	77
Total	5676.37	2370.5	–	182,577	113,102	–	–

Landsat-5 satellite imagery (Fig. 24), which indicates flooded locations by blue tone, enhanced by combining bands 5, 4, and 3.

*Validation of flood depth through sensitivity analysis of Manning’s n*

To evaluate the sensitivity to Manning’s *n* of flows in channel and immediate floodplain, an analysis was performed by considering Manning’s *n* values of each subdivision under cross-section 4 (yellow highlighted) and

corresponding 5-year return-simulated flood depth. With reference to cross-section 4, we have tried to correlate the simulated flood depth (Fig. 25a) with observed flood depth (Fig. 25b, and found slightly an underestimate (1–2 ft depth variation, Fig. 26) on both left and right over bank. However, HEC-RAS-simulated flood depth in channel, indicated between subdivisions 4–5, found good agreement with the observed data. It is important to remember that this Manning’s *n* sensitivity exercise was conducted using assumed peak flow (1100 m<sup>3</sup>/s) against a 10-year return period, while

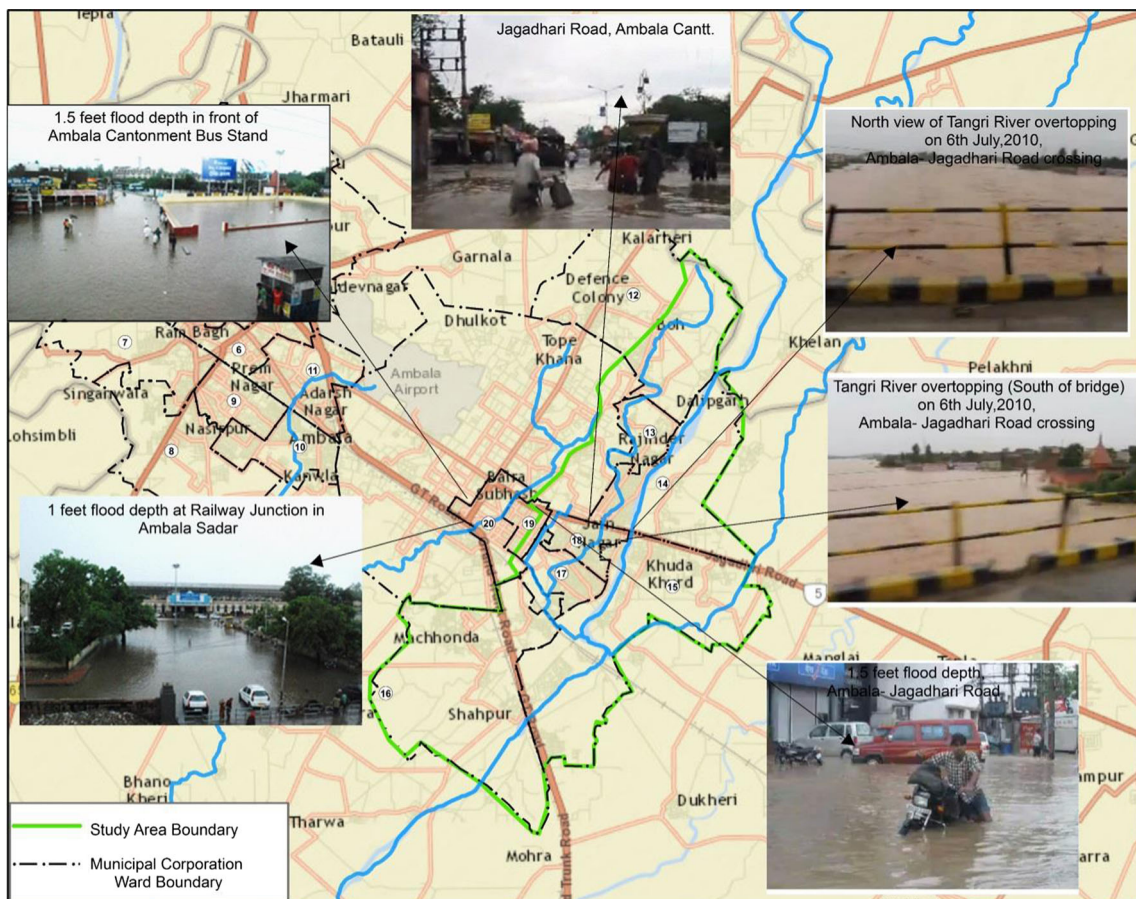
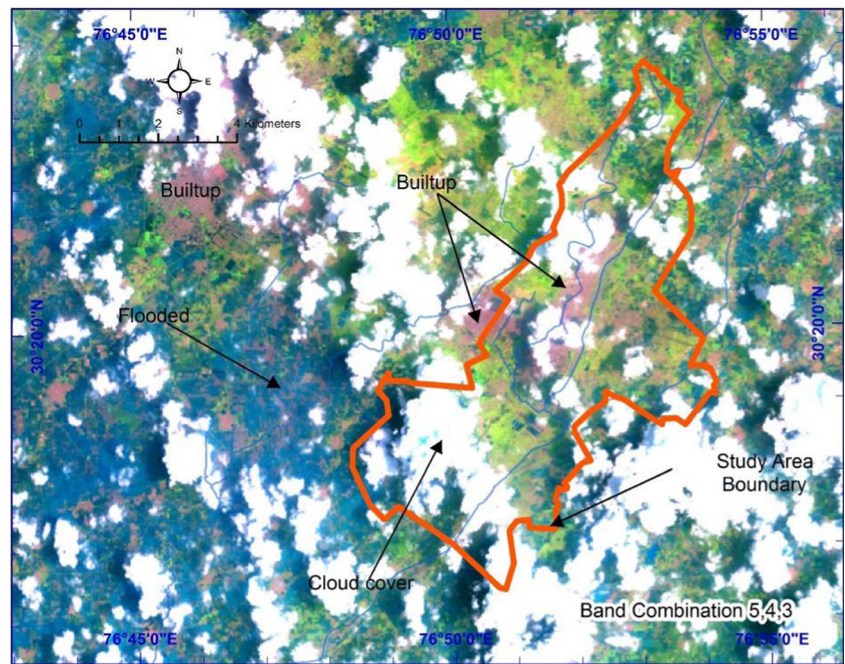


**Fig. 23** Flooding scenario during July 2010



**Fig. 24** TM Landsat-5 imagery shows flooded area in blue tone (TM Landsat-5 2010)



observed flood levels correspond to actual peak flow (1127 m<sup>3</sup>/s), as this was only available for the latest flood event of July 2010. We have not done calibration during simulation. Otherwise, this variation may be minimized. On the other side, this variation could be on account of local issues as explained in “Anthropogenic causes of flooding in urban areas,” as these play a considerable role in resistance of natural flows and resultant increasing flood depth. However, the HEC-RAS model was found to perform well in the calibration of Manning’s *n*. Even so, it is necessary

to further investigate sensitivity to the roughness parameter.

**Discussion and conclusion**

The present study has used a combination of the hydrological model (HEC-RAS) and GIS-based analytical framework to assess flood risk, and likely impact with a determined recurrence probability, calculated by frequency analysis. The most critical flood-prone sub-area (Ambala Sadar) in the Ambala

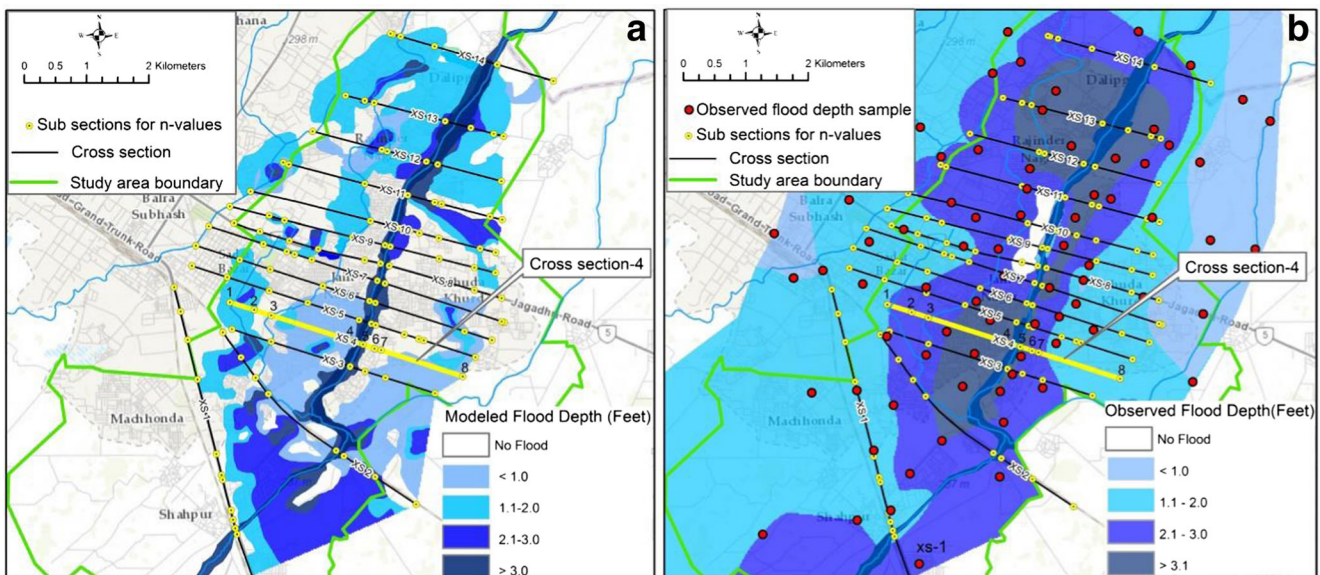
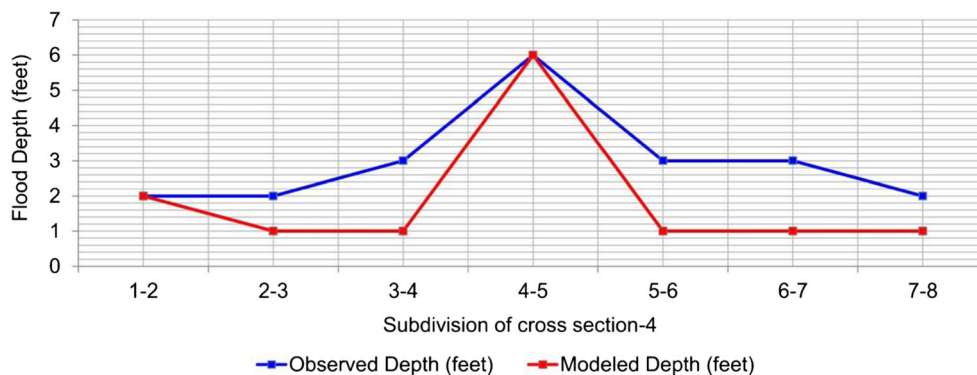


**Fig. 25** Manning’s *n* sensitivity test with reference to cross-section 4 (yellow highlighted) and corresponding HEC-RAS-simulated flood depth (a) and observed flood depth (b)

**Fig. 26** Comparison of HEC-RAS-simulated flood depth and observed flood depth corresponding to cross-section 4



City Municipal Corporation is selected as a case study. It is evident from the present study that in spite of inevitable natural factors, there are a number of anthropogenic causes, within and beyond city limit, which are responsible for resisting the free flow of runoff, leading to flooding problem. Considering the existing situation, flood inundation modeling is executed, and it shows that considerable flooding impact starts at a maximum discharge probability of 1000 m<sup>3</sup>/s against a 5-year return period, and the expected impact gradually increases with 10- and 20-year return flood. In terms of potential damage and land use vulnerability, the most likely affected areas belong to residential use, followed by commercial and public and semipublic use. Demographically, most flood-affected wards in descending order are 13, 19, 18, 15, 17, 14, and 16.

Generally, flood risk varies by site and situation, so in the case of Ambala City, on account of its location and hydro-meteorological characteristics, to some extent, flood risk is inevitable. In spite of these natural factors, with the advantage of flood-risk modeling using geospatial approach, the present study displayed that flood inundation modeling and resultant mapping can be used as a source for flood-risk management at city or municipality level in the following ways:

- It can help local authorities and agencies in determining location and allocation of land uses or development type, complying with different flood-risk zone while preparing for proposed local development plans.
- It allows the modeling of “what-if” scenarios for flood intensity and likely impact on population and infrastructure.
- These scenarios can help in formulating adaptation measures like access to critical facilities, rescue shelters, and evacuation routes.
- Such models can help in flood insurance studies and awareness generation among local people and stakeholders to avoid construction in core flood-risk zone.
- The present study is carried out for a small city with a small portion of the whole population, but the approach

and methodology can be generalized for larger urban areas.

**Acknowledgments** This paper is part of a PhD research thesis on the topic “Risk and Vulnerability Assessment of Flood Hazard in Ghaggar River Basin,” started in June 2010. Authors acknowledged the University Grant Commission (UGC), Ministry of Human Resource Development, Government of India, for financial support in carrying out the said work under major research project scheme recommended in January 2012. Authors are also grateful to the Municipal Corporation Ambala, Irrigation Department and Water Data Collection Division, Karnal, Government of Haryana for providing the necessary data. Authors also thank intermittent helpful discussions and technical supports provided by the faculty of the Department of Geography, Kurukshetra University, Kurukshetra, Haryana, India.

## References

- Adamowski K (1981) Plotting formula for flood frequency. *Water Resour Bull* 17(2):197–202
- Ahluwat J, Bansal R (2010) A report on floods management and drainage system in Haryana. Irrigation and Water Resources Department Haryana. <http://hid.gov.in/Docs/Paper%20on%20Floods.pdf>. Accessed 05 May 2012
- Aldridge BN, Garrett JM (1973) Roughness coefficients for stream channels in Arizona: U.S Geological Survey Open-File Report, p 87
- Alexander D (1991) Natural disasters: a framework for research and teaching. *Disasters* 15(3):209–226
- Ambala Municipal Corporation (2012), Directorate of Urban Local Bodies Department, Government of Haryana. <http://www.mcambala.gov.in/maps.aspx>. Accessed 12 March 2012
- Ambala District Disaster Management Plan (2012) Department of Revenue and Disaster, Government of Haryana
- Ambala District Disaster Management Plan (2015) Department of Revenue and Disaster Management, Government of Haryana
- Aphrodite N (2010) Hydrological assessment and modelling of the river Fani Catchment, Albania. Doctoral dissertation, Faculty of Advanced Technology, University of Glamorgan, Wales, UK
- Arora VK, Seglenisks F, Kouwen N, Soulis E (2001) Scaling aspects of river flow routing. *Hydrologic Process* 15(3):461–477
- Barnes HH (1967) Roughness characteristics of natural channels: U.S Geological Survey Water-Supply Paper (1849):213
- Brun SE, Band LE (2000) Simulating runoff behavior in an urbanizing watershed. *Comput, Environ Urban Syst* 24:5.22

- Buchele B, Kreibich H, Kron A, Thielen A, Ihringer J, Oberle P, Merz B, Nestmann F (2006) Flood-risk mapping: contributions towards an enhanced assessment of extreme events and associated risks. *Nat Hazards Earth Syst Sci* 6:485–503
- Carter RW, Einstein HA, Hinds Julian, Powel RW, Silberman E (1963) Friction factors in open channels, progress report of the task force on friction factors in open channels of the Committee on Hydro-mechanics of the Hydraulic Division: Proceedings, American Society of Civil Engineers. *J Hydraul Div* 89:97–143
- Casas A, Benito G, Thomdycraft V, Rico M (2006) The topographic data source of digital terrain models as a key element in the accuracy of hydraulic flood modelling. *Earth Surf Process Landf* 31:444–456
- Census of India (2011) Primary census abstract, the registrar general & census commissioner, ministry of home affairs, Government of India. <http://www.censusindia.gov.in/pca/pca.aspx>. Accessed 12 March 2015
- Chow VT (1959) *Open channel hydraulics*. McGraw-Hill, New York
- Cowan WL (1956) Estimating hydraulic roughness coefficients: *Agriculture Engineering* 37(7):473–475
- Crichton D (1999) The risk triangle. In: Ingleton J (ed) *Natural disaster management*. Tudor Rose, London, pp. 102–103
- Dempster GR (1974) Effects of urbanization on floods in the Dallas, Texas, metropolitan area: *US Geol. Survey Water Resour Inv*: 60–73
- DHI (2009) MIKE 11, A modeling system for rivers and channels, reference manual, Danish Hydraulic Institute, Denmark
- ESRI (2005) Arc Hydro Tools version 1.1, ESRI 380, New York St., Redlands, CA 92373-8100, USA
- FAO (1990) Guidelines for soil profile description. Third edition (revised), soil resources, management and conservation service. Land and Water Development Division, FAO, Rome
- Google Earth 6.1.0.5001 (2001, 2010, 2012, 2013) 30°18'0.37"N-30°43'18.28"N to 76°45'00"E-76°45'00"E-76°10'00"E, Historical imagery layer. <https://www.google.com/earth/>
- HARSAC (1997) Ghaggar watershed management using remote sensing data. A technical report by Haryana State Remote Application Centre, HARSAC/TR/07/97
- HEC-RAS v4.1 (2010) HEC-RAS v4.1 User Manual, US Army Corps of Engineers, Institute for Water Resources, Hydrologic Engineering Center (HEC), 609 Second Street, Davis, CA 95616-4687
- Helm P (1996) Integrated risk management for natural and technological disasters. *Tephra* 15(1):4–13
- Hirabayashi Y, Kanae S, Emori S, Kimoto M (2008) Global projections of changing risk of floods and droughts in a changing climate. *Hydrol Sci J* 53(4):754–773
- Hossain AKMA, Jia Y, Chao X (2009) Estimation of manning's roughness coefficient distribution for hydrodynamic model using remotely sensed land cover features. *Geoinformatics*. 635–638. <http://www.indiaenvironmentportal.org.in/files/file/Investment%20Climate.pdf>. Accessed 30 May 2016
- Investment Climate (2010) A report on northern states of India by Confederation of Indian Industry (CII)
- IPCC (2007) *Impacts, adaptation and vulnerability*. Cambridge University Press, Cambridge
- Irrigation Department Ambala (2012) SYL Water Service Circle Ambala, Irrigation and Water Resources Department, Government of Haryana
- Islam MM, Sado K (2000) Development of flood hazard maps of Bangladesh using NOAA-AVHRR images with GIS. *Hydrologic Sci-J-des Sci Hydrol* 45(3):337–355
- Jah A, Bloch R, Lamond J (2011) Cities and flooding, a guide to integrated urban flood risk management for the 21st century, pp. 199–202
- Johnson SL, Sayre DM (1973) Effects of urbanization on floods in the Houston, Texas metropolitan area: *U.S. Geol. Survey Water Resour Inv*: 3–73
- Kates RW, Wilbanks TJ (2003) Making the global local: responding to climate change concerns from the ground. *Environment* 45(3):12–23
- Khan SA (2007) Central Water Ground Board. Ground water information booklet-Ambala district, pp. 3–6
- Kron W (2005) Flood risk = hazard—values—vulnerability. *Water Int* 30:58–68
- Kumar R, Singh RD, Sharma KD (2005) Water resources of India. *Curr Sci* 89(5):800–801
- Kute S, Kakad S, Bhoje V, Walunj A (2014) Flood modeling of river Godavari using HEC-RAS. *Int J Res Eng Technol* 3:81–87
- Lumbroso D, Gaume E (2012) Reducing the uncertainty in indirect estimates of extreme flash flood discharges. *J Hydrol* (414–415) 16–30
- Mason DC, Cobby DM, Horritt MS, Bates PD (2003) Floodplain friction parameterization in twodimensional river flood models using vegetation heights derived from airborne scanning laser altimetry. *Hydrol Process* 17:1711–1732
- Mirza MMQ (2002) Global warming and changes in the probability of occurrence of floods in Bangladesh and implications. *Global Environ Change* 12:127–138
- National Disaster Management Guidelines (2010) Management of urban flooding. A Publication of the National Disaster Management Authority, Government of India. [http://www.ndma.gov.in/images/guidelines/management\\_urban\\_flooding.pdf](http://www.ndma.gov.in/images/guidelines/management_urban_flooding.pdf). Accessed on 07 August 2015
- National Remote Sensing Centre Hyderabad India (2013) Digital elevation model (30 m resolution) Cartosat-1 satellite. <http://bhuvan.nrsc.gov.in/data/download/index.php>. Accessed 28 August 2013
- Pappenberger F, Beven K, Horritt M, Blazkova S (2005) Uncertainty in the calibration of effective roughness parameters in HEC-RAS using inundation and downstream level observations. *J Hydrol* 302(1–4): 46–69
- Patil A (2015) Urban hydrology, need of India. *Environ We Int J Sci Technol* 10:29–36
- Patro S, Chatterjee C, Singh R, Raghuwanshi NS (2009) Hydrodynamic modelling of a large flood-prone river system in India with limited data. *Hydrol Process* 23:2774–2791
- Purba GS, Chakravorty B, Singh MK (2006) Identification of flood affected areas—need for a scientific approach. Working Group for Flood Control Programme for Xth Plan. <http://nidm.gov.in/idmc/proceedings/flood/b2%20-%202022.pdf>. Accessed 09 July 2015
- Ree WO (1954) *Handbook of channel design for soil and water conservation*: Soil Conservation Service, U.S. Department of Agriculture, SCS-TP-61, p 11
- Salimi S, Ghanbarpour MZ, Solaimani K, Ahmadi MZ (2008) Flood plain mapping using hydraulic simulation model in GIS. *J Appl Sci* 8(4):660–665
- Singh G, Babu R, Narain P, Bushan LS, Abrol IP (1992) Soil erosion rates in India. *J Soil Water Conserv* 47:97–99
- Skymet Weather Report (2015). Rain wreaks havoc in coastal districts. <http://www.skymetweather.com/content/weather-news-and-analysis/tamil-nadu-and-chennai-weather-update>. Accessed 26 November 2015
- Smith K (1996) *Environmental hazards: assessing risk and reducing disaster*, 2nd edn. Routledge, New York, USA
- Stenichon P (1997) Development and disaster management. *Austral J Emerg Manag Spring* 12(3):40–44
- Straatsma MW, Bapist MJ (2008) Floodplain roughness parameterization using airborne laser scanning and spectral remote sensing. *Remote Sens Environ* 112:1062–1080
- Subramanya K (2013) *Engineering hydrology*, 4th edn. Tata McGraw-Hill, New Delhi
- Syme WJ (2008) Flooding in Urban Areas-2D modeling approach for building and fences. *Engineers Australia*, 9th National Conference

- on hydraulic in water engineering, Darwin Convention Centre, Australia 23–26
- Tate E (1999) Introduction to HEC-RAS. Center for Research in Water Resources. <http://www.cer.utexas.edu/prof/maidment/grad/tate/research/RASExercise/webfiles/hecras.html#hydraulics>. Accessed 13 August 2015
- The Tribune (2007) Poor drainage to cause flooding again Punjab, Rajasthan generous with excess water. <http://www.tribuneindia.com/2007/20070629/harplus1.htm>. Accessed 06 July 2014
- The Tribune (2015) Why Chennai is going under. <http://www.tribuneindia.com/news/nation/why-chennai-is-going-under/165721.html>. Accessed 05 December 2015
- TM Landsat-5 (2010) NASA Landsat Program, Path/Row: 147/39, Scene ID: L5147039\_03920100715, Acquisition Date: Jul 15, 2010. <http://earthexplorer.usgs.gov/>. Accessed 03 August 2012
- Toutain O, Gopiprasad S (2006) Planning for urban infrastructure. India infrastructure report 2006. [http://www.iitk.ac.in/3inetwork/html/reports/IIR2006/Planning\\_for\\_Urban.pdf](http://www.iitk.ac.in/3inetwork/html/reports/IIR2006/Planning_for_Urban.pdf). Accessed 05 May 2015
- Town and Country Planning Department Haryana (2012) Development plans and notifications. <http://tcp.haryana.gov.in/>. Accessed 16 August 2013
- Tralli DM, Blom RG, Zlotnicki V, Donnellan A, Evans DL (2005) Satellite remote sensing of earthquake, volcano, flood, landslide and coastal inundation hazards. *ISPRS J Photogramm Remote Sens* 59:185–198
- UN DHA (1992) Internationally agreed glossary of basic terms related to disaster management. United Nations Department of Humanitarian Affairs (UN DHA), Geneva
- United Nations International Strategy for Disaster Reduction (2009). <http://www.unisdr.org/we/inform/publications/9413>. Accessed 07 August 2015
- USACE (2002) HEC-GeoRAS software, U.S Department of Defense, Army Corps of Engineers U.S., Institute for Water Resources, Hydrologic Engineering Center, 609 Second Street, Davis, CA. [http://www.hec.usace.army.mil/software/hecras/documentation/HEC-RAS\\_4.1\\_Reference\\_Manual.pdf](http://www.hec.usace.army.mil/software/hecras/documentation/HEC-RAS_4.1_Reference_Manual.pdf). Accessed 07 August 2014
- Van Aalst MK (2006) The impact of climate change on the risk of natural disasters. *Disasters* 30(1):5–18
- Weber A (2014) Within the edge: a revised approach to urban containment within the Chandigarh Periphery. Dissertation, College of Built Environments, University of Washington
- Whitfield PH (2012) Floods in future climates: a review. *J Flood Risk Manag* 5(4):336–365
- Wright NG, Villanueva PD, Bates DC, Mason MD, Pender WG, Neelz S (2008) Case study of the use of Remotely Sensed data for modeling flood inundation on the river Severn, UK. *J Hydraul Eng ASCE* 134(5):533–540